

Weights Shuffling for Improving DPSGD in Transformer-based Models

Jungang Yang
Shanghai Jiao Tong University
yangjungang@shu.edu.cn

Zhe Ji
Shanghai Jiao Tong University
ji_zhe@sjtu.edu.cn

Liyao Xiang
Shanghai Jiao Tong University
xiangliyao08@sjtu.edu.cn

Abstract—Differential Privacy (DP) mechanisms, especially in high-dimensional settings, often face the challenge of maintaining privacy without compromising the data utility. This work introduces an innovative shuffling mechanism in Differentially-Private Stochastic Gradient Descent (DPSGD) to enhance the utility of large models at the same privacy guarantee of the unshuffled case. Specifically, we reveal that random shuffling brings additional randomness to the trajectory of gradient descent while not impacting the model accuracy by the permutation invariance property — the model can be equivalently computed in both forward and backward propagations under permutation. We show that permutation indeed improves the privacy guarantee of DPSGD in theory, but tracking the exact privacy loss on shuffled model is particularly challenging. Hence we exploit the approximation on sum of lognormal distributions to derive the condition for the shuffled DPSGD to meet the DP guarantee. Auditing results show that our condition offers a DP guarantee quite close to the audited privacy level, demonstrating our approach an effective estimation in practice. Experimental results have verified our theoretical derivation and illustrate that our mechanism improves the accuracy of DPSGD over the state-of-the-art baselines on a variety of models and tasks.

I. INTRODUCTION

Recent work has revealed that trained neural networks pose great threats in leaking sensitive training data. Differential Privacy (DP) [14] serves both as a measure to quantify the upper bound of such information leak, and as mechanisms to ensure any individual sample’s impact on the model is negligible. The core principle of DP is to introduce random perturbation to the queried data, effectively preventing the disclosure of an individual sample. Differentially-private models have shown some defensive capability against privacy attacks including membership inference attacks [37], [38], [50], gradient matching attack [55], input reconstruction attack [8], etc.

Among the DP mechanisms, Differentially-Private Stochastic Gradient Descent (DPSGD) [1] emerges as an important one in privacy-preserving machine learning. By clipping the gradients of each example and inserting randomized noise to the clipped gradients in each training iteration, DPSGD ensures that the published model satisfies DP over the private training dataset. However, the conventional methods suffer significant accuracy losses due to the overwhelming amount of noise inserted, especially on deep and large models. Traditional DPSGD techniques, while effective in lower dimensions, struggle to maintain data utility as the model size enlarges.

Many works have been devoted into tackling the high-dimensional issue in DPSGD. Some have observed that the

gradients of deep neural networks mostly live on a very low dimensional manifold [41], [20], [30], and thus can be compressed without hurting the model performance too much. Based on the observation, a series of works [50], [51], [49], [54], [48] propose to replace the full gradients with their low-dimensional projection to reduce the overall noise added. Despite their impressive performance, most works avoid paying privacy price for the acquisition of low-dimensional representations, either by modifying the original model structure, or relying on auxiliary public data to estimate the low-dimensional projecting subspace. These works hardly keep the original training on large models as it is. Other works improve the accuracy of DPSGD by hyperparameters tuning [10], [31]. However, hyperparameters tuning consumes a great amount of computational resource in large-scale training. Moreover, such solutions merely provide training tricks which may not be transferable to other models.

We take a drastically different approach to mitigate the accuracy loss of DPSGD on large models — rather than blaming on the high dimensionality, we take advantage of it. As we observe, for large models, the possible number of weights permutations could be huge, *e.g.*, the permutation space for a billion-level model such as GPT-2 is as large as $10^9!$. Hence if we could randomly permute the model weights without affecting the model utility at each training step, we would obscure the training trajectory thus gaining privacy with no utility cost, alleviating the amount of additive perturbation noise.

One should note that there is a significant distinction between our methodology and the existing shuffle model of privacy [5], [15], [9], [4], [24], [16]. The latter is a distributed model in which a shuffler permutes the locally-differentially-private reports from different *users* for obfuscation. The shuffled reports are then released to a server for analysis. It has been shown that the random shuffling of inputs to locally private protocols amplifies the privacy guarantee [17]. In contrast, our approach works in the central DP scenario focusing on the shuffling of *model weights* instead of *user data* to hide the original weights among a set of weights which are equivalent in computing the output. The random shuffling enhances privacy as it obfuscates the training trajectories on the dataset hereby preserving training data privacy at a low accuracy cost. Moreover, we confront a unique challenge: the existing shuffle model of privacy naturally preserves accuracy as the user shuffling would not affect the computation, while a

naive random shuffling of model weights would totally destroy the model utility.

Fortunately, as we analyzed the mainstream neural architecture, we found that multilayer perceptron (MLP) and Transformer encoder blocks, both taking a large proportion of the model weights, satisfy permutation invariance property. Specifically, if their weight matrices are permuted, the permutation can be negated by an inverted permutation in the following layer without disrupting the forward and backward propagation. Hence weight permutation incurs zero accuracy loss on the inference or training of the model. Apart from that, MLP and Transformer encoder blocks widely exist in the state-of-the-art neural networks, especially large models with Transformer backbones, and these parts of a network are mostly dense, creating a huge space for permutation without any accuracy loss.

The primal challenge hence lies in *quantifying the privacy guarantee brought by random shuffling of model weights*. According to previous study [44], random shuffling introduces mixture distributions of which the tradeoff function is lower bounded by the unshuffled case, indicating higher indistinguishability of the former. However, the former works do not provide an explicit form of the privacy guarantee achieved by shuffling. To vividly explain why mixture distributions increase indistinguishability, we will show a toy example by mixture of Gaussians.

To better illustrate our intuition, we employ the Gaussian distribution as a toy example in Fig. 1. We have two points $(-2, 0)$ and $(2, 0)$ as the original data, the additive Gaussian mechanism generates outputs following distribution $\mathcal{N}((-2, 0), I)$ and $\mathcal{N}((2, 0), I)$ (left panel), respectively, providing plausible deniability in discriminating the two points. The closer the distance between the two distributions, the harder it is to discriminate. What shuffling does is to draw the two distributions closer by randomly permuting the data, i.e., the original $(2, 0)$ has a half of the chance to be revealed as $(0, 2)$. With the noise, the distribution $\mathcal{N}((2, 0), I)$ morphs into a Gaussian mixture centered at $(2, 0)$ and $(0, 2)$, and a Gaussian mixture is created for $\mathcal{N}((-2, 0), I)$ likewise. The measured distribution-wise distance is shorter between the Gaussian mixtures than that of the two original Gaussians, thereby enhancing the indistinguishability.

Yet, we encounter another challenge in accounting the privacy loss of the Gaussian mixtures which contain sum of log-normal distributions without a closed-form expression. We tackle the challenge by approximating the sum of log-normal distributions and provide an analytical condition to meet (ϵ, δ) -DP. Based on the condition, we propose the *shuffled DPSGD* mechanism, which takes one more step in each iteration of DPSGD: the gradients and weights of MLP and Transformer encoder blocks get randomly shuffled in each update. We compose the privacy loss over iterations by the advanced composition and amplify privacy by subsampling [40], as other accountant methods including moments accountant [1], RDP [32], GDP [12] have limitations on noise distributions apart from Gaussian.

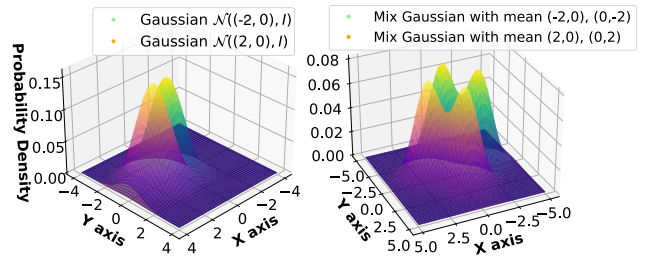


Fig. 1. Left: two Gaussian distributions. Right: the distributions after random shuffling. The $\mathcal{N}((-2, 0), I)$ turns into a Gaussian mixture distributed around $(-2, 0)$ and $(0, -2)$ and similarly for $\mathcal{N}((2, 0), I)$. We estimate the distributional distances by $\|P(x, y) - Q(x, y)\|_F$, where $\|\cdot\|_F$ means Frobenius norm, on an area $x, y \in [-10, 10]$. The measured distance on the left panel is 18.53 which is larger than 13.96 of the right panel.

We verify the permutation invariance property, and compare the performance of shuffled DPSGD with baselines on a variety of the state-of-the-art (large) models and tasks. We also audit our mechanism by the current auditing tool, showing that it indeed meets the privacy guarantee proposed. Experimental results demonstrate that the shuffled DPSGD leads to superior model accuracy to baselines at the same privacy level, especially when the privacy budget is tight (low ϵ s). From the implementation perspective, our shuffling mechanism incurs little overhead, readily to be deployed in the current DPSGD framework.

Highlights of our contribution are as follows. First, we theoretically prove that permutation of the outcome enhances the privacy guarantee, and propose the approximated condition for (ϵ, δ) -DP to hold in the shuffling case. Second, based on our theory and the permutation invariance property of neural networks, we propose *shuffled DPSGD* which improves the privacy guarantee over the conventional DPSGD. Finally, we verify our theory through experiments and show the efficacy of our design in the real-world large model private training.

II. RELATED WORK

Differentially-Private Stochastic Gradient Descent (DPSGD) is a method for protecting training data using differential privacy in machine learning [39], [1]. We will discuss the related works w.r.t. DPSGD.

DPSGD for natural language processing (NLP) tasks. Applying DPSGD to large models is hard in that the high dimensionality of the model often results in excessive amount of noise, leading to reduced model performance. Consequently, existing works have explored various approaches to enhance the accuracy of large models under differential privacy protection. For instance, studies [31], [2], [23], [48], [22] have focused on NLP tasks closely associated with large models. To reduce the memory costs of DPSGD in training large models, Li et al. introduced ‘ghost clipping’ [31], which significantly saves memory by fine-tuning the weight coefficients without instantiating each sample gradient. He et al. implemented a grouped and layered clipping mechanism [22], reducing the memory overhead of DPSGD while achieving

differentially-private training of GPT-3 model (with 175B parameters). Hoory et al. designed a differentially-private vocabulary algorithm [23], allowing training on a customized, domain-specific vocabulary while maintaining privacy. Yu et al. adopted classic compression methods in natural language processing (such as LoRA, Adapter, and Compacter) as ‘plugins’ [48], efficiently perturbing the compressed module instead to avoid overwhelming noise. By appropriately configuring hyperparameters such as batch size, learning rate, etc., Anil et al. conducted private pre-training [2], improving accuracy on masked language model BERT-Large (with approximately 340M parameters). These methods alleviate the accuracy degradation issue but alter either the original training process, or the original model, or the hyperparameter setting.

DPSGD for computer vision (CV) tasks. Studies [29], [50], [19], [10], [6] have primarily focused on large models in image processing tasks. Bu et al.’s work [6] extended the ‘ghost clipping’ [31] to convolutional neural networks (CNNs) like ResNet, reducing the computational overhead of DPSGD for CNNs. Another series of works focus on model reparametrization. Yu et al. decompose each weight matrix into the product of two low-rank matrices and a residual matrix [50], reducing the overall noise by perturbing only the gradients of the low-rank matrices. The noisy low-rank matrix gradients are then projected back to update the original weight matrices. However, this method still incurs high costs in weight reparametrization, and the noise could be amplified in projection, leading to significant accuracy losses. Golatkar et al. proposed an adaptive differential privacy algorithm [19], balancing data privacy and model accuracy by compressing private data gradients guided by public data gradient directions. Although such model compression-based works have improved efficiency/accuracy to some extent, they have deviated from the original large model training. In terms of hyperparameter configuration, De et al. found that the choice of hyperparameters in DPSGD is crucial to the training outcome [10] that, by selecting proper hyperparameters, their work achieves over 80% accuracy on the fine-tuned pre-trained NFNNet-F3 model on ImageNet. Similarly, Kurakin et al. improve accuracy of the deep ResNet model on ImageNet [29] by tuning hyperparameters.

Shuffle-DP. Since the proposal of the Encode, Shuffle, Analyze (ESA) system [5], the previous line of Shuffle-DP [15], [9], [4] has mainly focused on reducing the privacy budget of local differential privacy, where private data from different users gets shuffled by a trusted third-party aggregator, adding anonymity upon the original DP protection. That is to say, even in cases where the true value is uploaded, the adversary cannot pinpoint which one is the true value. Specifically, the anonymity brought by shuffling turns the original ϵ -DP into (ϵ', δ) -DP with $\epsilon > \epsilon'$, and such a privacy loss bound is further refined by works such as [16].

Our work follows a similar idea but takes a totally different approach. While Shuffle-DP primarily targets LDP, our work is designed for DPSGD and does not require a trusted third-party aggregator. We permute the model weights instead of shuffling

the dataset to get different sets of samples [24]. Moreover, the permutation brings additional computational issue in model training scenarios.

III. PRELIMINARIES

This section introduces the basic concepts and definitions fundamental to our study.

A. Differential Privacy

Differential Privacy (DP) is a framework for quantifying the privacy guarantees offered by a randomized mechanism. The definition of (ϵ, δ) -differential privacy provides a measure of the likelihood that an individual’s data can influence the output of an algorithm.

Definition 1 ((ϵ, δ) -Differential Privacy [14]). *A randomized mechanism M satisfies (ϵ, δ) -differential privacy if for any neighboring datasets X and X' differing by at most one unit, and for any possible output \mathcal{O} ,*

$$\Pr(\mathcal{M}(X) \in \mathcal{O}) \leq e^\epsilon \Pr(\mathcal{M}(X') \in \mathcal{O}) + \delta. \quad (1)$$

In the special case of $\delta = 0$, we call \mathcal{M} ϵ -differentially private.

We define l_2 -sensitivity on a pair of adjacent datasets which differ by a single record:

Definition 2 (l_2 -sensitivity). *The l_2 -sensitivity of the query function $f(X)$ is defined as*

$$s_2(f) = \sup_{d(X, X')=1} \|f(X) - f(X')\|_2,$$

where $\|\cdot\|_2$ is the l_2 norm.

DPSGD. In a deep learning task, the sensitive training dataset $X = [x_1, x_2, \dots, x_N]$ requires to be protected in T iterations of stochastic gradient descent. In each iteration, a batch of data B of size $|B|$ will be randomly selected to compute the gradient for weights $W : g = 1/|B| \sum_{x \in B} g(W, x)$, where $g(W, x)$ represents the gradient of the individual record x and the single g represents the average gradient of the batch. Since DP requires that the sensitivity of the outcome is bounded, conventional DPSGD conducts per-sample clipping on the gradients of each x :

$$\bar{g}(W, x) = g(W, x) / \max(1, \frac{\|g(W, x)\|_2}{C}), \quad (2)$$

to ensure that the sensitivity of the gradient, or clipping value is C , and thus the clipped batch gradient becomes $\bar{g} = 1/|B| \sum_{x \in B} \bar{g}(W, x)$. DPSGD mechanism \mathcal{M} inserts noise to the batch gradient: $\mathcal{M}(\bar{g}) = \bar{g} + \frac{1}{|B|}z$, where $z \sim \mathcal{N}(0, \sigma^2 C^2 I)$ has the same shape with \bar{g} . The standard deviation σ of the noise is a constant decided by the privacy budget (ϵ, δ) and C .

B. Model Structure

Here we give a detailed description of the common layer structures in large models, including MLP and Transformer encoder blocks.

Definition 3. We define MLP with two-layer linear projection as

$$x_{t+1} = h(x_t W_t^\top + b_t), \quad (3)$$

$$x_{t+2} = h(x_{t+1} W_{t+1}^\top + b_{t+1}), \quad (4)$$

where W_t and b_t is the weight and bias of t -th linear layer, W_{t+1} is the weight and bias of $(t+1)$ -th linear layer and $h(\cdot)$ is the activation function.

Definition 4. Standard transformer encoder block [42] is a popular building block for neural architectures, which contains multi-head attention and a MLP layer:

$$\text{Attention}(Q, K, V) = \text{softmax}\left(\frac{QK^\top}{\sqrt{d_k}}\right)V, \quad (5)$$

$$X_{t+1} = [A_1, \dots, A_h] W^O, \quad (6)$$

$$\text{where } A_i = \text{Attention}\left(X_t W_i^Q, X_t W_i^K, X_t W_i^V\right), \quad i \in [h]. \quad (7)$$

The projections are parameter matrices $W_i^Q \in \mathbb{R}^{d_m \times d_k}$, $W_i^K \in \mathbb{R}^{d_m \times d_k}$, $W_i^V \in \mathbb{R}^{d_m \times d_v}$ and $W^O \in \mathbb{R}^{hd_v \times d_m}$. W^O means the output weight matrix, and d_m, d_k, d_v are the dimensions of the model, key, and value, respectively.

We will prove the parameter permutation invariance under the shuffle mechanism on these two types of layers.

C. Sum of Log-Normal Distribution

Lemma 1 (F-W approximation of sum of lognormal distributions [18]). Given d i.i.d. normal distributions $Y_i \sim \mathcal{N}(\mu_i, \sigma^2)$ for $i = 1, \dots, d$. The sum of d log-normal random variables $S_d = \sum_{i=1}^d e^{Y_i}$ can be approximated by:

$$S_d \approx e^Y, \quad \text{where } Y \sim \mathcal{N}(\mu_Y, \sigma_Y^2), \quad (8)$$

given that

$$\sigma_Y^2 = \log \left[(e^{\sigma^2} - 1) \frac{\sum_{i=1}^d e^{2\mu_i}}{\left(\sum_{i=1}^d e^{\mu_i}\right)^2} + 1 \right], \quad (9)$$

$$\mu_Y = \log \left[\sum_{i=1}^d e^{\mu_i} \right] + \frac{\sigma^2}{2} - \frac{\sigma_Y^2}{2}. \quad (10)$$

D. Privacy Accountant

To track the privacy loss in DPSGD, Moments Accountant [1] and Renyi Differential Privacy Accountant [32] are commonly used. These methods accumulate the logarithm of the moments of privacy loss at each step, but have the drawback of overestimating the privacy budget [26]. Therefore, Sivakan

et al. proposed the Privacy loss Random Variables (PRVs) Accountant in [21], outperforming other accountant schemes in the context of DPSGD. This method truncates and discretizes the Privacy Loss Random Variables (PRVs), and then uses Fast Fourier Transform (FFT) to efficiently convolve the distributions of the PRVs. Adapted from the PLD Accountant [26], [27], [25], the PRV Accountant solves the problem in PLD Accountant that it cannot compose differentially-private algorithms. However, the PRV Accountant is still limited in that it cannot be applied to random variables of any distribution. Taking generalizability and tightness of the bound into account, we choose advanced composition [40] in this work:

Theorem 1 (Advanced Composition, Thm. 22 in [40]). For $j \in [k]$, letting $M_j : \mathcal{X}^n \times \mathcal{Y}_{j-1} \rightarrow \mathcal{Y}_j$ be the randomized algorithm which is $(\varepsilon_j, \delta_j)$ -DP, we inductively define $M_{1\dots j} : \mathcal{X}^n \rightarrow \mathcal{Y}_j$ by $M_{1\dots j}(x) = M_j(x, M_{1\dots(j-1)}(x))$, where $M_{1\dots 0}(x) = y_0$ for some fixed $y_0 \in \mathcal{Y}_0$. Then $M_{1\dots k}$ is (ε, δ) -DP for any $\delta > \sum_{j=1}^k \delta_j$ with

$$\varepsilon = \min \left\{ \sum_{j=1}^k \varepsilon_j, \frac{1}{2} \sum_{j=1}^k \varepsilon_j^2 + \sqrt{2 \log(1/\delta') \sum_{j=1}^k \varepsilon_j^2} \right\}, \quad (11)$$

where $\delta' = \delta - \sum_{j=1}^k \delta_j$.

This Theorem provides a general composition method that can be applied to any differential privacy mechanism. It is not limited to any specific distribution, and thus we apply it in our proposed method to calculate the privacy budget.

Moreover, we apply the Privacy Amplification by Subsampling (Thm. 29 in [40]) to amplify the privacy budget by batch sampling:

Theorem 2 (Privacy Amplification by Subsampling). For dataset $x \in \mathcal{X}^n$, let $x_U \in \mathcal{X}^n$ denote the entries of x indexed by $U \subset [n]$ which is a random subset. That is, $(x_U)_i = x_i$ if $i \in U$ and $(x_U)_i = \perp$ if $i \notin U$, where $\perp \in \mathcal{X}$ is some null value. Given $M : \mathcal{X}^n \rightarrow \mathcal{Y}$ satisfying (ε, δ) -DP, we define $M^U : \mathcal{X}^n \rightarrow \mathcal{Y}$ by $M^U(x) = M(x_U)$. Let $p = \max_{i \in [n]} \mathbb{P}[i \in U]$. Then M^U is (ε', δ') -DP for $\varepsilon' = \log(1 + p(e^\varepsilon - 1))$ and $\delta' = p \cdot \delta$.

This theorem could be applied to amplify the privacy budget of each step in DPSGD, where the random subset U represents the batch sampled.

IV. METHODOLOGY

This section delineates our approach. We begin with the motivation of using shuffling to reinforce privacy, illustrate our shuffling mechanism, and then provide the differential privacy guarantee of shuffled Gaussian — a Gaussian mechanism with post shuffling.

Motivation. From the entropy perspective, shuffling would increase the ambiguity of the outcome, thereby enhancing the privacy strength of the input. Specifically, shuffling increases the randomness in data processing by rearranging elements

of the (noisy) output, which disrupts the potential relation between the output and its private input, therefore reducing reliance on the randomness of the additive perturbation noise. The result is a relaxed constraint on the perturbation noise at the same level of privacy guarantee.

We take the Gaussian mechanism as an example for a deeper analysis. A Gaussian mechanism composed by random shuffling is interpreted as a mixture of Gaussian, where each shuffled noisy output appears with a certain probability. Random shuffling turns a single-spike (Gaussian) distribution into a multi-spike (mixture of Gaussian) one where each spike has a reduced magnitude compared to the single spike. Thus the transformation from a Gaussian into a mixture of Gaussian can be considered as distribution smoothing, making adjacent distribution pairs harder to distinguish.

Meanwhile, it is also crucial to prevent shuffling to affect the actual SGD procedures: no accuracy price should be paid for shuffling. We will show how we achieve this in the following section.

A. The Shuffling Mechanism

Although the shuffling of the outcome would bring additional randomness, we need to carefully implement it to avoid any model performance decline. Inspired by the permutation equivariance property [46], we propose a weight shuffling mechanism that does not alter the forward and backward propagation. Our definition of permutation invariance is as follows:

Definition 5 (Weights Permutation Invariance). *For a model $f(W, x)$ with weights W and input x , the permutation-invariant set \mathcal{P}_s is defined as*

$$\mathcal{P}_s = \{P \mid f(W, x) = f(P(W), x), \forall x\} \quad (12)$$

where the permutation P denotes a mapping from a set to itself with a permuted order.

Provided the definition, we now show two widely used network structures are permutation-invariant.

Theorem 3 (MLP Permutation Invariance). *Let $W = \{W_t, W_{t+1}, b_t, b_{t+1}\}$ be the parameters of MLP defined in Def. 3, and $x = x_t$ be the input to the MLP. For any element-wise activation function $h(\cdot)$ like ReLu, tanh and Softmax, MLP $f(W, x)$ is permutation-invariant in both the forward and backward propagation if the following permutation is applied:*

$$P(W) = \{P_1^\top W_t, b_t P_1, W_{t+1} P_1, b_{t+1}\}, \quad (13)$$

where P_1 is any permutation matrix.

The proof can be obtained by calculation, and we place it in Appendix A.

Theorem 4 (Transformer Permutation Invariance). *Let $W = \{W_i^K, W_i^Q, W_i^V, W_i^O\}$ for $i \in [h]$ with h heads be the parameters of the transformer block defined in Def. 4. For any element-wise activation function $h(\cdot)$ like ReLu, tanh and Softmax, the transformer block is permutation-invariant in*

both the forward and backward propagation if the following permutation is applied:

$$P(W) = \{W_i^K P_{1i}, W_i^Q P_{1i}, W_i^V P_2, P_3 W_i^O\}, \quad (14)$$

where $P_{1i} \in \mathbb{R}^{d_k \times d_k}$, $P_2 \in \mathbb{R}^{d_v \times d_v}$, and

$$P_3 = \begin{bmatrix} P_2^\top & 0 & \cdots & 0 \\ 0 & P_2^\top & \cdots & 0 \\ \vdots & \vdots & \ddots & \vdots \\ 0 & 0 & \cdots & P_2^\top \end{bmatrix} \in \mathbb{R}^{hd_v \times hd_v} \quad (15)$$

are any permutation matrices.

We also refer readers to the proof in Appendix B.

Although we merely define permutation invariance on two network structures, the two structures widely exist in all types of neural networks. Particularly, the transformer block constitutes a major component of the popular Transformer-based large models. Hence a vast majority of the current large models could permute all or a part of their parameters without altering their outputs by Thm. 3 and 4.

Randomized shuffling. Since any permutation from \mathcal{P}_s can be chosen to apply to the model weights without changing the output, we sample a permutation across all elements in \mathcal{P}_s by a uniform distribution. Therefore, all analysis is based on that the permutation is *uniformly* sampled from \mathcal{P}_s in the following. We start from a simple case of shuffling a vector to analyze how random shuffling impacts the output distribution, with Gaussian mechanism as an instance.

We discuss how shuffling is integrated with a vectorized Gaussian mechanism. In the conventional Gaussian mechanism, a zero-centered Gaussian noise vector is added to the output vector (of the same size) to achieve DP. Our shuffled Gaussian mechanism only takes one more step.

Definition 6 (Shuffled Gaussian). *A uniformly chosen random permutation $P \in \mathcal{P}_s$ turns vector $y \in \mathbb{R}^d$ into vector $P(y) \in \mathbb{R}^d$. The shuffled Gaussian is defined as $\mathcal{M}(y) = P(y) + z$, where $z \sim \mathcal{N}(\mathbf{0}, \sigma^2 I) \in \mathbb{R}^d$. Letting the outcome be the random variable $o = P(y) + z$, its probability density function (PDF) is*

$$p(o) = \frac{1}{|\mathcal{P}_s|} \sum_{i=1}^{|\mathcal{P}_s|} \frac{1}{(2\pi\sigma^2)^{|\mathcal{P}_s|/2}} e^{-\frac{\|o - y^{(i)}\|_2^2}{2\sigma^2}}, \quad (16)$$

where $y^{(i)}$ is the i -th permutation of y and $|\mathcal{P}_s|$ denotes the total number of permutations which meet Def. 5.

Without causing confusion, we use P to both denote a deterministic permutation as well as a random variable on \mathcal{P}_s . In the shuffled Gaussian mechanism, the original output vector is first rearranged by a permutation which is randomly sampled from \mathcal{P}_s , and then is added a zero-centered Gaussian noise vector. Notably, the PDF of Eq. 16 remains the same if we choose to add noise before shuffling the noisy vector. This is because the Gaussian noise z is i.i.d. in each dimension.

B. Shuffling Improves Privacy

A vital point in our motivation is that the output distribution gets smoother and the distribution-wise distance gets shorter by the shuffling mechanism. In shuffled Gaussian, we consider the shuffling mechanism a post-processing step of the Gaussian mechanism, and the shuffling mechanism does not access the original data. Therefore, the shuffled Gaussian must at least satisfy the DP that the pure Gaussian mechanism provides. In this section, we give the proof that shuffled Gaussian indeed improves the privacy guarantee of the Gaussian mechanism.

Theorem 5 (Comparison with Gaussian mechanism). *The privacy guarantee δ of the Shuffled Gaussian is smaller than or equal to that of the Gaussian mechanism under the same ϵ for meeting (ϵ, δ) -DP.*

Proof. According to Def. 6, the output distributions of the queries on x and x' are

$$P[f(x)] + z \triangleq Y = \left\{ Y^{(i)} \text{ w.p. } \frac{1}{a}, \right. \quad (17)$$

$$Y^{(i)} \sim \mathcal{N}(f^{(i)}(x), \sigma^2 I), i \in [a], \quad (18)$$

$$P[f(x')] + z \triangleq Y' = \left\{ Y'^{(i)} \text{ w.p. } \frac{1}{b}, \right. \quad (19)$$

$$Y'^{(i)} \sim \mathcal{N}(f^{(i)}(x'), \sigma^2 I), i \in [b]. \quad (20)$$

We use a, b to denote the number of different permutations of $f(x), f(x')$, respectively. Let $q(y) = \frac{1}{(2\pi\sigma^2)^{d/2}} e^{-\frac{\|y\|^2}{2\sigma^2}}$ be defined as the probability density function (PDF) of the d -dimensional Gaussian distribution $\mathcal{N}(0, \sigma^2 I_d)$. Then the probability density functions of Y and Y' , denoted as $p(y)$ and $p'(y)$, can be written as follows:

$$\begin{aligned} p(y) &= \frac{1}{a} \sum_{i=1}^a q(y - f^{(i)}(x)) \\ &= \frac{1}{a} \sum_{i=1}^a \frac{1}{(2\pi\sigma^2)^{d/2}} e^{-\frac{\|y - f^{(i)}(x)\|_2^2}{2\sigma^2}} \triangleq \frac{1}{a} \sum_{i=1}^a q_i(y), \end{aligned} \quad (21)$$

$$p'(y) = \frac{1}{b} \sum_{i=1}^b q(y - f^{(i)}(x')) \triangleq \frac{1}{b} \sum_{i=1}^b q'_i(y),$$

Here, we define $q_i(x) = q(y - f^{(i)}(x))$ and $q'_i(x) = q(y - f^{(i)}(x'))$. For any adjacent datasets, the query outputs satisfying differential privacy is equivalent to having

$$\begin{aligned} \Pr(P[f(x)] + z \in O) - e^\epsilon \Pr(P[f(x')] + z \in O) &\leq \delta \\ \Leftrightarrow \delta &= \sup_O \int_O p(y) - e^\epsilon p'(y) dy, \end{aligned} \quad (22)$$

$$\Leftrightarrow \delta = \int_{O^*} \frac{1}{a} \sum_{i=1}^a q_i(y) - e^\epsilon \frac{1}{b} \sum_{i=1}^b q'_i(y) dy \quad (23)$$

where $O^* = \{y \mid p(y) - e^\epsilon p'(y) \geq 0\}$. Letting k be the least

common multiple of a and b , we have

$$\begin{aligned} \delta &= \int_{O^*} \left[\frac{1}{k} \sum_{i=1}^k q_i(y) - e^\epsilon \frac{1}{k} \sum_{i=1}^k q'_i(y) \right] dy \\ &= \int_{O^*} \frac{1}{k} \sum_{i=1}^k [q_i(y) - e^\epsilon q'_i(y)] dy \\ &= \frac{1}{k} \sum_{i=1}^k \int_{O_i^*} [q_i(y) - e^\epsilon q'_i(y)] dy \quad (24) \\ &\leq \frac{1}{k} \sum_{i=1}^k \int_{O_i^*} [q_i(y) - e^\epsilon q'_i(y)] dy \\ &\leq \frac{1}{k} \sum_{i=1}^k \delta_0 = \delta_0. \end{aligned}$$

O_i^* is defined as $\{y \mid q_i(y) - e^\epsilon q'_i(y) \geq 0\}$ for all i , and δ_0 is the largest δ among all pure Gaussian mechanisms defined on O_i^* , which are the same in the unshuffled case. Hence it is evident that the privacy guarantee improves by shuffling. \square

C. Privacy Guarantee of Shuffled Gaussian

Although Sec. IV-B provides evidence that shuffling improves the privacy guarantee, it is still unclear how much improvement presented and how one can manipulate that in practice. In this section, we offer a more precise, tighter privacy guarantee for the shuffled Gaussian:

Theorem 6 (Privacy Guarantee of Shuffled Gaussian). *Given query function $f(x) \in \mathbb{R}^d$ on any adjacent datasets X, X' , and the Gaussian noise $z \sim \mathcal{N}(\mathbf{0}, \sigma^2 I) \in \mathbb{R}^d$, the shuffled Gaussian $\mathcal{M}(f(x))$ satisfies (ϵ, δ) -differentially private if*

$$\Phi\left(\frac{\sigma_{Z_1}}{2} + \frac{\zeta_1 - \epsilon}{\sigma_{Z_1}}\right) - e^\epsilon \Phi\left(\frac{\sigma_{Z_2}}{2} + \frac{\zeta_2 - \epsilon}{\sigma_{Z_2}}\right) \leq \delta, \quad (25)$$

where Φ is the CDF of the standard Gaussian distribution, and

$$\begin{aligned} \zeta_1 &= -\log(1 + (d-1)e^{-\frac{d\epsilon c'}{(d-1)\sigma^2}}), \\ \zeta_2 &= -\log(1 + (d-1)e^{-\frac{d\epsilon(c+c')}{(d-1)\sigma^2}}) - \frac{c^2}{\sigma^2}, \\ \sigma_{Z_1}^2 &= \log \left[\frac{1 + (d-1)e^{-\frac{2d\epsilon c'}{(d-1)\sigma^2}}}{(1 + (d-1)e^{-\frac{d\epsilon c'}{(d-1)\sigma^2}})^2} (e^{\frac{c^2}{\sigma^2}} - 1) + 1 \right], \\ \sigma_{Z_2}^2 &= \log \left[\frac{1 + (d-1)e^{-\frac{2d\epsilon(c+c')}{(d-1)\sigma^2}}}{(1 + (d-1)e^{-\frac{d\epsilon(c+c')}{(d-1)\sigma^2}})^2} (e^{\frac{c^2}{\sigma^2}} - 1) + 1 \right], \end{aligned} \quad (26)$$

where $\|f(x) - f(x')\|_2 \leq c$, $\|f(x)\|_2 \leq c'$.

The detail of the computation and the proof are collected in Appendix C. Here we present a sketch proof.

Proof. At the beginning, a special case needs to be excluded from discussion, namely, $f(x)$ and $f(x')$ are both equal-entry vectors where random shuffling cannot properly work, i.e., the vector does not change after shuffling. The case is almost

impossible to occur and is degraded to the unshuffled case. Hence we ignore the special case.

We start from simplifying the criterion of O^* in Eq. (23) as follows.

$$p(y) - e^\epsilon p'(y) \geq 0 \quad (27)$$

$$\Leftrightarrow \frac{\frac{1}{k} \sum_{i=1}^k e^{-\|y-f^{(i)}(x)\|_2^2/(2\sigma^2)}}{\frac{1}{k} \sum_{i=1}^k e^{-\|y-f^{(i)}(x')\|_2^2/(2\sigma^2)}} \geq e^\epsilon, \quad (28)$$

where k is the least common multiple of a and b . We define the difference between the adjacent queries as $g = f(x') - f(x)$, and for convenience, we abbreviate $f^{(i)}(x)$ as $f^{(i)}$. Then Eq. (28) can be written as

$$\frac{\frac{1}{k} \sum_{i=1}^k e^{\langle y, f^{(i)} \rangle / \sigma^2}}{e^{-(\|g\|_2^2 + 2\langle f, g \rangle) / (2\sigma^2)} \frac{1}{k} \sum_{i=1}^k e^{\langle y, f^{(i)} \rangle + \langle y, g^{(i)} \rangle / \sigma^2}} \geq e^\epsilon, \quad (29)$$

By Lemma 3 (with a proof in Appendix C), a sufficient but not necessary condition for the output $y \in O^*$ is

$$e^{-\epsilon + (\|g\|_2^2 + 2\langle f, g \rangle) / (2\sigma^2)} \geq \sum_{i=1}^k e^{\langle y, g^{(i)} \rangle / \sigma^2}. \quad (30)$$

With the inequality, we can derive a lower bound for δ as

$$\delta = \int_{O^*} \frac{1}{k} \sum_{i=1}^k q_i(y) - e^\epsilon \frac{1}{k} \sum_{i=1}^k q'_i(y) dy \quad (31)$$

$$\geq \frac{1}{k} \sum_{i=1}^k \left[\Pr \left[\sum_{j=1}^k e^{\langle Y^{(i)}, g^{(j)} \rangle / \sigma^2} \leq C(\epsilon) \right] \right] \quad (32)$$

$$- \frac{1}{k} \sum_{i=1}^k \left[e^\epsilon \Pr \left[\sum_{j=1}^k e^{\langle Y^{(i)}, g^{(j)} \rangle / \sigma^2} \leq C(\epsilon) \right] \right] \quad (33)$$

where $C(\epsilon) = e^{-\epsilon + (\|g\|_2^2 + 2\langle f, g \rangle) / (2\sigma^2)}$. The term $\sum_{j=1}^k e^{\langle Y^{(i)}, g^{(j)} \rangle / \sigma^2}$ is a typical sum of log-normal distributions as $\langle Y^{(i)}, g^{(j)} \rangle = \mathcal{N}(\langle f^{(i)}, g^{(j)} \rangle, \|g\|_2^2 \sigma^2)$ and such a distribution does not have an explicit probability density function. Thus we apply Lemma 1 to approximate it as a log-normal distribution:

$$\sum_{j=1}^k e^{\langle Y^{(i)}, g^{(j)} \rangle / \sigma^2} \approx e^{Z_1}, \quad Z_1 \sim \mathcal{N}(\mu_{Z_1}, \sigma_{Z_1}^2), \quad (34)$$

$$\sigma_{Z_1}^2 = \log \left[\frac{\sum_{j=1}^k e^{2\mu_{ij}}}{\left(\sum_{j=1}^k e^{\mu_{ij}} \right)^2} \left(e^{\frac{\|g\|_2^2}{\sigma^2}} - 1 \right) + 1 \right], \quad (35)$$

$$\mu_{Z_1} = \log \left(\sum_{j=1}^k e^{\mu_{ij}} \right) + \frac{\|g\|_2^2}{2\sigma^2} - \frac{\sigma_{Z_1}^2}{2}; \quad (36)$$

where $\mu_{ij} = \frac{\langle f^{(i)}, g^{(j)} \rangle}{\sigma^2}$. Therefore, the probability distribution in Eq. (32) can be approximated as follows:

$$\Pr \left[\sum_{j=1}^k e^{\langle Y^{(i)}, g^{(j)} \rangle / \sigma^2} \leq C(\epsilon) \right] \approx \Pr \left[e^{\mathcal{N}(\mu_{Z_1}, \sigma_{Z_1}^2)} \leq C(\epsilon) \right], \quad (37)$$

$$= \Pr \left[\mathcal{N}(\mu_{Z_1}, \sigma_{Z_1}^2) \leq \log C(\epsilon) \right] = \Phi \left(\frac{\log C(\epsilon) - \mu_{Z_1}}{\sigma_{Z_1}} \right) \quad (38)$$

$$= \Phi \left(\frac{\zeta_1 - \epsilon}{\sigma_{Z_1}} + \frac{\sigma_{Z_1}}{2} \right), \quad \text{where } \zeta_1 = -\log \left(\sum_{j=1}^k e^{\mu_{ij}} \right) + \frac{\langle f, g \rangle}{\sigma^2}. \quad (39)$$

We define $\mu'_{ij} = \frac{\langle f^{(i)}(x'), g^{(j)} \rangle}{\sigma^2}$, and σ_{Z_2}, ζ_2 by replacing μ_{ij} with μ'_{ij} in σ_{Z_1}, ζ_1 , respectively. By approximating the probability distribution in Eq. (33) similarly, we have

$$\Pr \left[\sum_{j=1}^k e^{\langle Y^{(i)}, g^{(j)} \rangle / \sigma^2} \leq C(\epsilon) \right] \quad (40)$$

$$- e^\epsilon \Pr \left[\sum_{j=1}^k e^{\langle Y^{(i)}, g^{(j)} \rangle / \sigma^2} \leq C(\epsilon) \right] \quad (41)$$

$$\approx \Phi \left(\frac{\sigma_{Z_1}}{2} + \frac{\zeta_1 - \epsilon}{\sigma_{Z_1}} \right) - e^\epsilon \Phi \left(\frac{\sigma_{Z_2}}{2} + \frac{\zeta_2 - \epsilon}{\sigma_{Z_2}} \right) \triangleq h(\sigma_{Z_1}, \sigma_{Z_2}). \quad (42)$$

Finally, we estimate δ by deriving the upper bound for $h(\sigma_{Z_1}, \sigma_{Z_2})$ which is an approximated lower bound to δ . To this end, we establish the following lemma by analyzing the property of h :

Lemma 2. *Given the definition of $\sigma_{Z_1}^2, \sigma_{Z_2}^2, \zeta_1, \zeta_2$ and the constraints $\|g\|_2 \leq c, \|f\|_2 \leq c'$, $h(\sigma_{Z_1}, \sigma_{Z_2})$ achieves the upper bound at $k = d$, where*

$$f = \sqrt{\frac{1}{d(d-1)}} c' [(d-1), -1, \dots, -1], \quad (43)$$

$$g = \sqrt{\frac{1}{d(d-1)}} c [(d-1), -1, \dots, -1]. \quad (44)$$

Here f and g share the maximum value at the same dimension, not necessarily the first one. Thereby one can derive the condition of Eq. (25) and Eq. (26).

The detailed proof of the lemma is provided in Appendix D, which mainly takes advantage of the monotonicity of h . \square

Note that Thm. 6 is obtained at the worst case where the total number of invariant permutations $|\mathcal{P}_s|$ is the least (except for the case where all elements are the same). In general, to have the same (ϵ, δ) -DP held, the shuffled Gaussian requires a declining noise magnitude σ with the increase in the total number of permutations k , or the dimensionality of the vector d . In fact, the noise variance σ^2 in the shuffled Gaussian is approximately $O\left(\frac{1}{\log d}\right)$. The result is interesting in indicating a lower level of privacy budget (ϵ, δ) is required

for the same amount of noise (σ) applied, illustrating shuffling indeed makes the output distributions harder to distinguish, and the higher the query dimension, the more difficult the discrimination.

In the following section, we will discuss how shuffling mechanism could be applied to DPSGD. It should be noted that although the theorems we give here is based on the vector form, the conclusion can be easily extended into matrix form by reshaping matrices into vectors with one-to-one correspondence.

V. SHUFFLED DPSGD

In this section, we introduce the shuffled DPSGD mechanism, including the algorithmic detail, the privacy loss accountant, and its DP guarantee.

A. The Algorithm

Shuffled DPSGD mostly follows the framework of DPSGD but introduces shuffling to the permutation-invariant part of the neural network at each weights update. Hence the privacy of gradients or weights in each iteration is amplified through shuffling without accuracy decay. Alg. 1 for integrating the shuffling mechanism into DPSGD involves several key steps. The first step is to randomly initialize the model parameters W_0 . In each iteration, a random sample batch L_t is selected with probability $|B|/N$, where $|B|$ is the batch size and N is the total number of samples. Then the per-sample gradients of L_t are computed and clipped to ensure that the sensitivity of each gradient is c . This per-example gradient clipping step aligns with that of the normal DPSGD and ensures the condition of $\|f(x) - f(x')\|_2 \leq c$ is satisfied in Thm. 6. The clipped gradients are accumulated by batch, and the noise is added to the accumulated gradients. An additional batch clipping (line 12) is required to meet the constraint of $\|f(x)\|_2 \leq c'$ in Thm. 6.

As illustrated in the following section, we calculate the noise variance σ^2 by $|B|, c, N$, training steps T and ε, δ by the specific privacy accountant we choose. Here we apply Advanced Composition and Privacy Amplification by Subsampling for the accounting. If the noise variance σ^2 is higher than the noise variance σ_0^2 calculated by DPSGD, the algorithm will fall back to the original implementation of DPSGD. Otherwise, a random shuffling step would be added upon noise addition before weights update. It is worth noting that the random shuffling does not impact the weight update as the permutation invariance property holds not only in the forward but also in the backward propagation, according to Thm. 3 and 4.

Notably, we choose to add noise before shuffling ($P(y+z)$) instead of after shuffling ($P(y) + z$) in Alg. 1. The former is more convenient in that we do not need to shuffle the corresponding weights apart from permuting the gradients. The two are equivalent as $P(y+z) = P(y)+P(z)$, $P(z) \sim \mathcal{N}(\mathbf{0}, \sigma^2 I)$ following the same distribution of z . This indicates $P(y+z)$ has the same distribution with $P(y) + z$. Hence the change does not alter the privacy guarantee.

Algorithm 1 Shuffled DPSGD

Input: (a) Training dataset X , (b) privacy budget ε, δ , (c) model weights W . (d) clipping value c , batch clipping value c' , batch size $|B|$, total N examples, total T training steps.

Output: Private model weights W_{T+1} .

- 1: Initialize W_0 randomly
 - 2: Compute σ for shuffled-DPSGD by advanced composition and subsampling.
 - 3: Compute σ_0 for DPSGD by advanced composition and subsampling.
 - 4: **for** $t \in [T]$ **do**
 - 5: Sample $L_t \in X$ with sampling probability $|B|/N$
 - 6: **for** $i \in [L_t]$ **do**
 - 7: Compute $\mathbf{g}_t(x_i) \leftarrow \nabla_{W_t} \mathcal{L}(W_t, x_i)$
 - 8: $\bar{\mathbf{g}}_t(x_i) \leftarrow \mathbf{g}_t(x_i) / \max\left(1, \frac{\|\mathbf{g}_t(x_i)\|_2}{c}\right)$
 - 9: **end for**
 - 10: Accumulate the clipped gradients over a batch $\hat{\mathbf{g}}_t = \sum_i^{|B|} \bar{\mathbf{g}}_t(x_i)$
 - 11: **if** $\sigma < \sigma_0$ and W_t is linear layer or Transformer block **then**
 - 12: Clip the batch gradient $\bar{\mathbf{g}}_t = \hat{\mathbf{g}}_t / \max\left(1, \frac{\|\hat{\mathbf{g}}_t\|_2}{c'}\right)$
 - 13: Add noise $\tilde{\mathbf{g}}_t = \frac{1}{|B|} (\bar{\mathbf{g}}_t + z)$, where $z \sim \mathcal{N}(0, \sigma^2 c^2 I)$
 - 14: $W_{t+1} \leftarrow P[W_t - \eta_t \tilde{\mathbf{g}}_t]$
 - 15: **else**
 - 16: Add noise $\tilde{\mathbf{g}}_t = \frac{1}{|B|} (\hat{\mathbf{g}}_t + z)$, where $z \sim \mathcal{N}(0, \sigma_0^2 c^2 I)$
 - 17: $W_{t+1} \leftarrow W_t - \eta_t \tilde{\mathbf{g}}_t$
 - 18: **end if**
 - 19: **end for**
 - 20: **return** W_{T+1}
-

B. Privacy Budget Accountant

In assessing the privacy cost of DPSGD, the Moments Accountant [1], and the Renyi Differential Privacy (RDP) Accountant [32] are widely recognized methods. These approaches accumulate the logarithm of the moments of the privacy loss variable at each iteration. However, they cannot accurately estimate the privacy budget for the shuffled DPSGD due to the incompatibility of the two accountant methods with the computation involving mixture of Gaussian. Specifically, these algorithms both require an exponential parameter, denoted as α in RDP and λ in Moments Accountant. The issue emerges when α or λ is a non-integer, leading to difficulties in expressing the PDF of the mixture of Gaussian. Even for integers, it demands the trouble to calculate multivariate expansions for the exponential parameter. All these complications hinder us from adopting their accountant methods.

We have also considered privacy accountant methods such as PLDs [26] and PRVs [27]. However, these techniques also encounter issues in computing Gaussian mixture. For example, the PRVs method optimizes the privacy budget by

subsampling, but it produces results that are contradictory to the expected behavior of Gaussian mixture, yielding higher privacy costs under fixed noise. This is mainly due to the Fast Fourier Transform (FFT) transformation is designed for Gaussian distribution, not applicable for the composition of Gaussian mixture.

Therefore, we consider a general composition method that is irrelevant to the underlying noise distribution. Hence we adopt the Advanced Composition from Thm. 1 and the Privacy Amplification by Subsampling from Thm. 2 together for calculating the privacy budget per training step. Specifically, we set an identical privacy budget across all training steps, i.e., $\epsilon_j = \epsilon_s, \delta_j = \delta_s, \forall j \in [k]$. The sampling rate $p = |B|/N$. By substituting $\epsilon = \epsilon_s, \delta = \delta_s$ into Eq. (25), we can compute the noise variance σ^2 required for each training step under shuffling.

VI. EXPERIMENTS

We verify the theorems and evaluate the performance of the shuffled DPSGD in this section. The experiments are designed to address the following key research questions: (1) Does the shuffling mechanism guarantee weights permutation invariance? (2) How does the F-W method perform in approximating the sum of log-normal distributions? (3) What is the relationship among σ, ϵ, d in the shuffled setting? (4) How does the accuracy of large models improve by Shuffled DPSGD? (5) How does Shuffled DPSGD perform under auditing? (6) What is the overhead introduced by the shuffling mechanism? The answers to these questions are listed from Sec. VI-B to Sec. VI-G.

A. Experimental Setup

Models, datasets and tasks. We conduct comprehensive experiments on a range of models, datasets, and tasks in both CV and NLP fields. The first category of tasks is CV classification, the second being NLP classification and the third one is text generation. For CV classification, we train ViT [13] to classify the CIFAR-100 [28] dataset. For NLP classification tasks, we employ two models BERT[11] and RoBERTa on four datasets: stanford sentiment treebank (SST-2), quora question pairs (QQP), Question Natural Language Inference (QNLI), and MultiNLI (MNLI) from the GLUE benchmark [43]. For the text generation task, we use GPT-2 and GPT-2-large [36] to generate text given E2E [35] and DART [33] datasets. ViT is pre-trained on ImageNet, whereas the rest models are adopted from the pre-trained ones in the Huggingface library. We summarize the configuration and training/fine-tuning hyperparameters in Table I.

Metrics. For the classification tasks of CV and NLP, we use the testing accuracy as the evaluation metric. To verify the weights permutation invariance of the shuffling mechanism, we additionally include loss as the metric. As to the text generation tasks, BLEU and Meteor are employed as the evaluation metrics. Except for the loss, a higher value indicates a better performance for all metrics.

Baselines. We introduce the state-of-the-art works on DPSGD as baselines, which are Ghost clipping [31] and MixOpt [7]. Ghost clipping and MixOpt are algorithmically optimized for per-sample gradient calculation based on Opacus [47] library. Opacus is a popular pytorch-based DPSGD code platform, which is continuously updated, and offers three different privacy accountant methods: RDP, GDP and PRV. RDP accountant is adopted in our experiments as the accountant method for all baselines. In ghost clipping, the per-sample gradients is clipped without being instantiated, thus saving both running time and memory costs. MixOpt method is further improved from Book-Keep [6] (A variant of ghostclipping) and provides a lighter running time overhead than Book-Keep.

Implementation details. We run the experiments on Nvidia GeForce RTX 3090 GPU except for training GPT-2 large on Nvidia A100 GPU. The implementation is Pytorch-based. Baselines are reproduced in their respective environments. In the hyperparameter setting of all NLP tasks, we set the clipping value to 0.1, and fix δ to $1/(2N)$ where N is the number of training samples in each dataset. For CV tasks, we set the clipping value to 1, and fix $\delta = 5 \times 10^{-6}$. Other hyperparameters are listed in Table I.

Shuffle implementation. For the implementation of the shuffling mechanism, we perform permutation by creating random row and column indices for each weight matrix, instead of directly performing matrix multiplications. This can greatly reduce the time overhead of which the results can be found at Sec. VI-G. The code detail is provided in Appendix E.

B. Verifying Permutation Invariance

We first show the permutation invariance holds by conducting experiments to compare the difference in weights trained under shuffling and that without shuffling. We fix the random seed for a straightforward comparison. By calculating the ℓ_2 norm of the weights difference pre- and post-shuffling on ViT, we observed a significant discrepancy of 1063.02, showing that the shuffling mechanism induces substantial perturbation in the model weights.

Meanwhile, we verify permutation invariance by training ViT on CIFAR100 and Bert on SST-2 in both non-private mode and differentially-private mode. The same noise multiplier σ (equivalent to $\epsilon = 1$ in normal DPSGD) is applied and the random seed is fixed. The training results with or without shuffling are listed in Table II, showing exactly the same test loss and accuracy with shuffling or not. It is evidenced that applying the proposed shuffling mechanism results in zero difference between the shuffled and original model, indicating that the model is trained equivalently under shuffling.

C. Sum of Lognormal Approximations

We empirically evaluate the approximation error of the F-W method [18] used in our mechanism, and compare it with different approximation methods including Monte-carlo method, S-Y method, LSQ method [52] and KDE method [3].

TABLE I
MODEL CONFIGURATIONS AND TRAINING HYPERPARAMETERS. SHUFFLE RATIO MEANS THE PROPORTION OF THE WEIGHTS THAT ARE SHUFFLED BY OUR MECHANISM IN THE MODEL.

Model	#Trainable Param	Shuffle Ratio	Dataset	#Train Samples N	Learning Rate	Epochs	δ
ViT	85.8M	100%	CIFAR100	50,000	2×10^{-3}	10	5×10^{-6}
BERT	110M	100%	SST-2	67,349	5×10^{-4}	3	$1/(2N)$
RoBERTa	125M	100%	QQP	363,846	5×10^{-4}	18	$1/(2N)$
			MNLI	392,702	5×10^{-4}	18	$1/(2N)$
			QNLI	108,000	5×10^{-4}	6	$1/(2N)$
GPT-2	124M	100%	E2E	42,043	0.002	10	8×10^{-6}
GPT-2-large	0.838B	100%	DART	60,591	5×10^{-4}	15	10^{-5}

TABLE II
VERIFYING PERMUTATION INVARIANCE ON ViT AND BERT IN NON-PRIVATE AND DPSGD MODES.

Method	non-private		shuffled non-private		DPSGD		shuffled with same σ	
	test loss	test accuracy	test loss	test accuracy	test loss	test accuracy	test loss	test accuracy
ViT	0.6362	89.68%	0.6362	89.68%	1.330	85.56%	1.330	85.56%
BERT	0.2302	92.31%	0.2302	92.31%	1.054	87.38%	1.054	87.38%

TABLE III
ACCURACY (%) COMPARISON OF SHUFFLED DPSGD, GHOST CLIPPING AND MIXOPT ON CIFAR-100 CLASSIFICATION TASKS. THE OPTIMAL PERFORMANCE IS MARKED IN BOLD.

Model	$\epsilon = 0.1$			$\epsilon = 0.5$			$\epsilon = 1$			
	Non-private	Ghost	MixOpt	Shuffled-DPSGD	Ghost	MixOpt	Shuffled-DPSGD	Ghost	MixOpt	Shuffled-DPSGD
ViT	89.68	1.20	1.26	67.31	72.99	72.98	75.17	75.53	75.55	75.61

TABLE IV
ACCURACY (%) COMPARISON OF SHUFFLED DPSGD, GHOST CLIPPING AND MIXOPT ON NLP CLASSIFICATION TASKS. THE OPTIMAL PERFORMANCE IS MARKED IN BOLD.

Model	Datasets	Non-private	$\epsilon = 0.1$			$\epsilon = 0.5$			$\epsilon = 1$		
			Ghost	MixOpt	Shuffled-DPSGD	Ghost	MixOpt	Shuffled-DPSGD	Ghost	MixOpt	Shuffled-DPSGD
BERT	SST-2	92.32	69.27	64.56	87.5	86.58	87.38	88.42	88.19	86.93	88.30
	QQP	90.49	69.51	69.73	82.14	80.85	80.51	82.25	83.39	82.07	82.26
	MNLI	83.27	55.65	55.58	73.04	70.33	70.12	73.05	73.52	73.25	73.07
	QNLI	89.51	51.29	59.69	81.49	81.03	81.64	82.04	81.77	81.82	81.78
RoBERTa	SST-2	94.95	87.50	87.62	92.32	90.82	92.08	91.63	91.86	91.62	91.51
	QQP	91.50	68.19	68.28	83.59	80.67	80.51	83.37	83.39	83.20	83.35
	MNLI	87.49	55.11	53.03	79.29	78.14	78.01	79.21	79.78	79.84	79.38
	QNLI	93.56	73.86	73.86	85.67	85.22	85.92	85.94	85.59	86.14	85.76

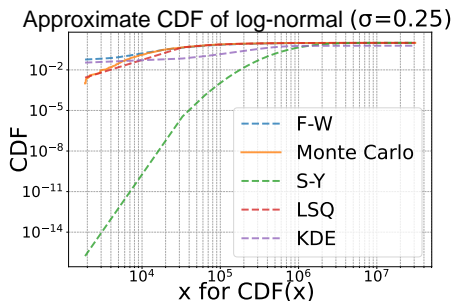


Fig. 2. The comparison of different approximation methods for the sum of log-normal distribution. We set $\sigma = 0.25$ and dimension $d = 10^8$ to depict its CDF curve.

Monte-carlo method calculates the sum of randomly sampled log-normal variables and repeats the procedure for 1000 times to depict the CDF curve. S-Y method computes the distribution for the sum of log-normal iteratively. It first computes the distribution for the sum of two log-normal random variables, and then adds the third one up to compute the new distribution. The summation goes iteratively until all d log-normal random variables are summed up. LSQ method leverages the least squares method to fit the sum of log-normal distributions, whereas KDE method adopts the Gaussian kernel density estimation method to fit the sum of log-normal distributions.

Here we consider the Monte-carlo method to be the closest to the groundtruth distribution, but the method demands a very large number of samples to give an accurate estimate. For

example, sampling 1000 points for $d = 10^8$ took 62 minutes, which is hardly fit for DPSGD. Except for the F-W method, all other methods are numerical without any analytical form of the CDF. Furthermore, the LSQ and KDE methods both depend on sampling which is too heavy-weighted even if cutting down the number of samples.

The results are shown in Fig. 2. As we can see, the F-W method approximation of the sum of log-normal distribution is sufficiently close to the ‘ground truth’ (Monte-carlo). S-Y method provides poor performance at a lower value. Although the LSQ method and KDE method have better performance, they require sampling similar to Monte-carlo and do not have a closed-form expression. Therefore, we conclude that the F-W method is the best choice for the approximation of the sum of log-normal in our design.

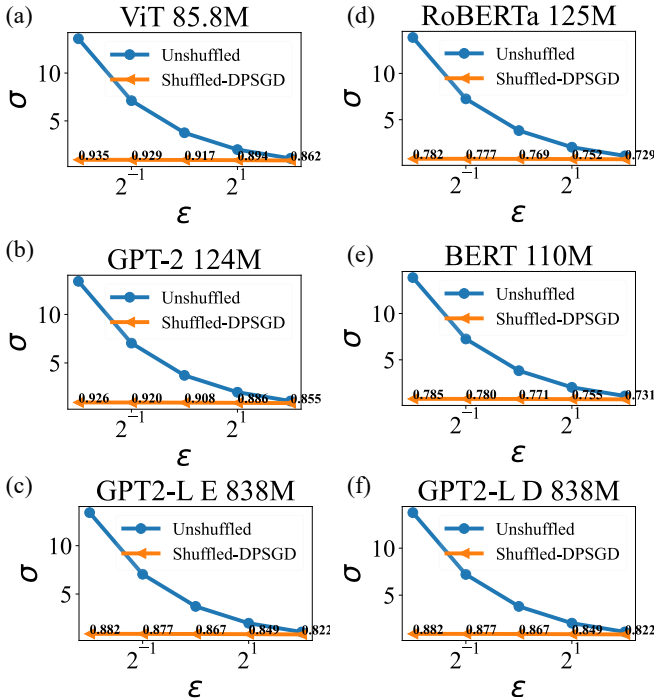


Fig. 3. Comparison of the relations between σ and ϵ in both unshuffled and shuffled DPSGD. For (a)-(e) we calculate different σ s with $\epsilon \in \{0.25, 0.5, 1, 2, 4\}$. And ‘‘GPT2-L E’’ represent the GPT-2-large model trained with E2E dataset and ‘‘GPT2-L D’’ represent the GPT-2-large model trained with DART dataset.

D. Relations of $\sigma, \epsilon, & d$

The theoretical relations of σ, ϵ, d provided in Thm. 6 is too complicated to tell straightforwardly. Hence we numerically show how the three key parameters interact in the real settings.

Due to space limitation, we only display results of six representative experiments, each with parameter size $d = 85.8\text{M}, 110\text{M}, 125\text{M}, 124\text{M}, 838\text{M}$, respectively. The $\sigma - \epsilon$ curves are depicted in Fig. 3. We observe that the shuffling mechanism has a significant impact on the privacy accountant of DPSGD across all model sizes. From the figure, the σ s almost flattened out across different ϵ s in shuffled mechanism, leaving other factors like d to blame for its change in values.

As we focus on the high privacy regime (ϵ as low as 0.25), we observe that, the σ in the shuffled DPSGD is merely 5-7% of that of the unshuffled.

It may be attributed to that the noise magnitude σ at the order $O(1/\sqrt{\log d})$, which is very small at extremely large d s. We can tell that d mainly appears along with $e^{\frac{1}{\sigma^2}}$ as $(d-1)e^{-\frac{d}{(d-1)\sigma^2}}$ in σ_{Z_i}, ζ_i , where $i = 1, 2$. Therefore, if the model’s dimension reaches 10^9 , the σ is dominated by d but not by the ϵ .

For a more straightforward demonstration, we show the heatmap in Fig. 4 to present the relations of ϵ, σ and dimensionality for shuffled DPSGD. The column of $d = 1$ represents the σ of an unshuffled mechanism. In the unshuffled case, σ increases fast with the decrease of ϵ . However, as dimensionality d increases, σ drops drastically and the change in ϵ barely affects σ . Therefore, in the shuffled case, d becomes the major impact factor to the value of σ .

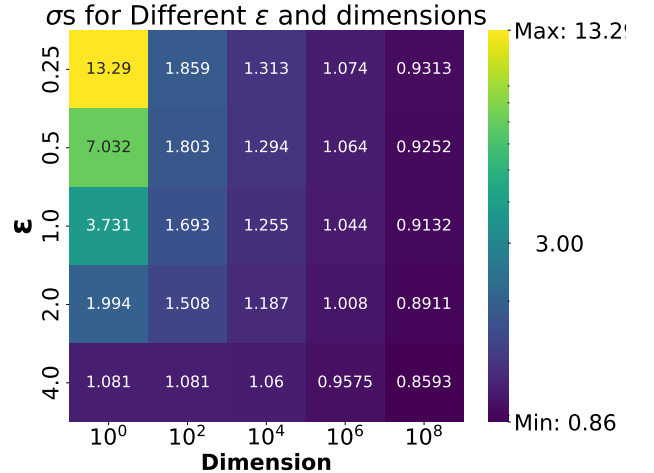


Fig. 4. The σ s from the unshuffled ($d = 1$) and shuffled DPSGD under different ϵ s and d s.

E. Performance of Shuffled DPSGD

We evaluate the real-world performance of shuffled DPSGD in comparison with the baselines on large-scale models. The results are reported according to the categories of the tasks.

CV Classification. The setup of ViT follow the ViT checkpoint google/vit -base-patch16-224 from Hugging-face transformers library [45], pretrained on ImageNet-21k and fine-tuned on ImageNet (also referred to as ILSVRC2012). Since this pre-trained model is very powerful, easily reaching over 96% accuracy under all circumstances on CIFAR-10, we hence omit the results but select a more difficult task — 100-class classification on CIFAR-100 — for performance test. The results in Table III show that our shuffled DPSGD consistently outperforms all baselines under various ϵ s, and the improvement is more significant at small ϵ values. Particularly, at $\epsilon = 0.1$ where both Ghost clipping and MixOpt have performance close to random guesses, shuffled DPSGD enjoys a high accuracy well over 60%.

TABLE V
COMPARISON OF SHUFFLED DPSGD, GHOST CLIPPING AND MIXOPT ON GPT-2 AND GPT-2-LARGE. THE OPTIMAL PERFORMANCE IS MARKED IN BOLD.

Models	Datasets	Non-private	$\varepsilon = 0.1$			$\varepsilon = 0.5$			$\varepsilon = 1$		
			Ghost	MixOpt	Shuffled-DPSGD	Ghost	MixOpt	Shuffled-DPSGD	Ghost	MixOpt	Shuffled-DPSGD
GPT-2	DART(BLEU)	62.00	1.91	0.92	38.73	23.71	33.51	40.56	40.94	32.49	42.68
	DART (METEOR)	0.474	0.005	0.008	0.333	0.298	0.318	0.3612	0.356	0.341	0.3859
	E2E (BLEU)	66.75	0.18	0.01	45.93	35.80	44.79	49.77	53.80	46.29	54.93
	E2E (METEOR)	0.4537	0.0201	0.0108	0.3119	0.2877	0.3091	0.3286	0.3328	0.3174	0.3436
GPT-2-large	DART(BLEU)	66.28	5.74	4.73	53.45	47.28	46.27	54.77	52.36	52.63	53.97
	DART (METEOR)	0.521	0.073	0.045	0.4570	0.423	0.418	0.4791	0.449	0.450	0.4936
	E2E (BLEU)	68.80	0.21	0.09	63.46	30.97	33.82	64.51	45.42	45.55	65.02
	E2E (METEOR)	0.4625	0.0549	0.0487	0.3986	0.2410	0.2590	0.4195	0.3180	0.3231	0.4276

However, such an improvement becomes marginal at large ε s. As we analyze, this is mostly due to the inexact approximation of F-W method at small σ s. In Thm. 6, the variance of per normal distribution in the sum of log-normals is approximated as $\frac{c^2}{\sigma^2}$, which grows with small σ s. As stated in [53], the F-W approximation method is quite accurate when the variance of log-normal distributions is low but becomes less accurate at a high variance. Hence, at small σ s, or large ε s, the power of the approximation approach diminishes.

NLP Classification. We finetune a raw BERT checkpoint `bert-base-uncased` and a RoBERTa checkpoint `roberta-base` in a differentially-private way for NLP classification, in which both pre-trained models are available in the Huggingface library. The results under all cases are presented in Table IV. The trend is similar to CV classification, as our method almost always achieves higher accuracy than baselines at the same privacy level. Notably, our accuracy is merely 1 – 4% shy of the non-private case, showing great applicability of our method to privacy-preserving NLP tasks. In fact, in NLP tasks, quite different from the CV task, the accuracy of our method is only mildly affected by the ε value. This reflects the results of Sec. VI-D where ε 's impact on σ gets weakened in the high-dimensional case.

Table-To-Text Generation. We fine-tune the pre-trained model checkpoint `gpt2` and `gpt2-large` from Huggingface in a differentially-private way. The results are reported in Table V. It can be found that the performance of the shuffled DPSGD is far superior to baselines, especially at $\varepsilon = 0.1$. This is in line with the analysis that the accuracy performance of our method is less affected by the limited privacy budget thanks to shuffling. It is also clear that the performance gap between the shuffled DPSGD and the non-private method is smaller on GPT-2-large compared to GPT-2. In fact, at $\varepsilon = 1$, the performance of our method on GPT-2-large is very close to that of the non-private case, demonstrating that our shuffling approach enjoys a unique advantage on large models, verifying the intuition that the shuffled DPSGD benefits from high-dimensional model weights.

F. Privacy Auditing of Shuffled DPSGD

So far, our privacy accountant relies on some relaxations and approximations. We would like to see how our mechanism acts

TABLE VI
AUDITING RESULTS OF SHUFFLED DPSGD ON ViT, CIFAR100.

Theoretical ε	0.5	1.0
Audited ε	0.4771	0.7005

against real-world auditing. Hence we implement the auditing method for DPSGD in [34], which presents the most recent progress in DPSGD auditing as far as we know. We conduct auditing tests in the training of ViT on CIFAR-100 under the theoretical $\varepsilon = 0.5, 1$ by shuffled DPSGD. A total of 10,000 training steps is performed to get the records through ‘white-box access with gradient canaries.’ The setup of ‘Dirac canary: All gradient values are zero except at a single index’ in [34] is reused in our test with a batch size 1000 and epoch number 200 to get sufficient observations.

We apply the auditing method to the shuffled DPSGD and obtain the auditing ε s as

$$\varepsilon = \max \left\{ \ln \left(\frac{1 - \alpha - \delta}{\beta} \right), \ln \left(\frac{1 - \beta - \delta}{\alpha} \right), 0 \right\} \quad (45)$$

where α and β represent the type I error and type II error, respectively. We compare the empirical ε s with the theoretical values in Table VI. For $\varepsilon = 0.5$, we eliminate cases where $\alpha < 4 \times 10^{-4}$ and $\beta < 4 \times 10^{-4}$ to mitigate the impact of inaccurate measurement of the small probability events. The audited ε is a reasonably close lower bound to the theoretical counterparts.

This indicates that our privacy accountant for shuffled DPSGD provides reasonably accurate estimations. However, there is still a discrepancy between the theoretical and empirical ε values, which can be attributed to the approximations in the theoretical analysis and the fact that the audited privacy level is mostly a lower bound to the actual privacy level. Nevertheless, considering the limited observations (10^4), the auditing results is acceptable as the gap between the audited and the theoretical upper bound is not closed in [34] either.

G. Overhead of Shuffled DPSGD

We compare the overhead of shuffling under different implementations: index operations (our approach), matrix multiplication (`torch.mm`), and sparse matrix multiplication

TABLE VII
TIME COSTS OF DIFFERENT SHUFFLING IMPLEMENTATIONS.

method	Times(ms)
Index shuffle	0.9799
Matrix multiplication	1316.6
Sparse matrix multiplication	322.62

TABLE VIII
AVERAGE EPOCH TIME OF RUNNING SHUFFLED DPSGD.

Model	Unshuffled	Shuffled
ViT, CIFAR	2min25s	2min42s
BERT, QNLI	28min28s	28min53s
RoBERTa, QNLI	29min45s	30min11s
GPT-2, E2E	30min1s	30min13s
GPT-2-large, E2E (on A100)	43min25s	44min29s

(`torch.sparse.mm`) in randomly shuffling a $10,000 \times 10,000$ matrix. We found that index operations greatly save the running time, which is about 0.1% of that by matrix multiplication and 0.3% of that by sparse matrix multiplication. The results are in Table VII.

The overall computational overhead of shuffled DPSGD is measured by the average epoch running time as reported in Table VIII. All experiments are conducted on a single RTX 3090 GPU except for GPT-2 large. We can see that the additional overhead of shuffling is under 30 seconds except for GPT-2-large, which is 64 seconds, mostly due to its billion-level parameters and the enormous permutation space. Nevertheless, the shuffling overhead takes only 2.3% of the overall training time in shuffled DPSGD, which is almost negligible in training.

VII. CONCLUSION

We developed the theoretical condition for (ϵ, δ) -DP to hold under shuffled Gaussian mechanism. Based on the theory, we proposed shuffled DPSGD, a method that enhances the accuracy of DPSGD by incorporating a shuffling mechanism to reduce the additive noise, thus boosting the overall model performance. Our shuffling mechanism, designed to maintain weights permutation invariance, is adaptable to a variety of up-to-date neural networks. Experimental results confirmed our findings, and showed that shuffled DPSGD significantly improves performance over baselines on large models, highlighting its lightweighted implementation and running time overhead.

REFERENCES

[1] M. Abadi, A. Chu, I. Goodfellow, H. B. McMahan, I. Mironov, K. Talwar, and L. Zhang, "Deep Learning with Differential Privacy," in *Proceedings of the 2016 ACM SIGSAC Conference on Computer and Communications Security (CCS)*. ACM, 2016, pp. 308–318.

[2] R. Anil, B. Ghazi, V. Gupta, R. Kumar, and P. Manurangsi, "Large-scale differentially private bert," in *Conference on Empirical Methods in Natural Language Processing*, 2021.

[3] Ö. Askin, T. Kutta, and H. Dette, "Statistical quantification of differential privacy: A local approach," in *43rd IEEE Symposium on Security and Privacy, SP 2022, San Francisco, CA, USA, May 22-26, 2022*. IEEE, 2022, pp. 402–421. [Online]. Available: <https://doi.org/10.1109/SP46214.2022.9833689>

[4] B. Balle, J. Bell, A. Gascón, and K. Nissim, "The privacy blanket of the shuffle model," in *Advances in Cryptology – CRYPTO 2019*, A. Boldyreva and D. Micciancio, Eds. Cham: Springer International Publishing, 2019, pp. 638–667.

[5] A. Bittau, U. Erlingsson, P. Maniatis, I. Mironov, A. Raghunathan, D. Lie, M. Rudominer, U. Kode, J. Tinnes, and B. Seefeld, "Prochlo: Strong privacy for analytics in the crowd," in *Proceedings of the 26th Symposium on Operating Systems Principles*, ser. SOSP '17. New York, NY, USA: Association for Computing Machinery, 2017, p. 441–459. [Online]. Available: <https://doi.org/10.1145/3132747.3132769>

[6] Z. Bu, J. Mao, and S. Xu, "Scalable and efficient training of large convolutional neural networks with differential privacy," in *Advances in Neural Information Processing Systems 35: Annual Conference on Neural Information Processing Systems 2022, NeurIPS 2022, New Orleans, LA, USA, November 28 - December 9, 2022*, 2022. [Online]. Available: http://papers.nips.cc/paper_files/paper/2022/hash/fa5617c176e76fee83f3f9947fd9f3f-Abstract-Conference.html

[7] Z. Bu, Y. Wang, S. Zha, and G. Karypis, "Differentially private optimization on large model at small cost," in *International Conference on Machine Learning, ICML 2023, 23-29 July 2023, Honolulu, Hawaii, USA*, ser. Proceedings of Machine Learning Research, A. Krause, E. Brunskill, K. Cho, B. Engelhardt, S. Sabato, and J. Scarlett, Eds., vol. 202. PMLR, 2023, pp. 3192–3218. [Online]. Available: <https://proceedings.mlr.press/v202/bu23a.html>

[8] N. Carlini, C. Liu, Ú. Erlingsson, J. Kos, and D. Song, "The secret sharer: Evaluating and testing unintended memorization in neural networks," in *28th USENIX Security Symposium, USENIX Security 2019, Santa Clara, CA, USA, August 14-16, 2019*, N. Heninger and P. Traynor, Eds. USENIX Association, 2019, pp. 267–284.

[9] A. Cheu, A. Smith, J. Ullman, D. Zeber, and M. Zhilyaev, "Distributed differential privacy via shuffling," in *Advances in Cryptology – EURO-CRYPT 2019*, Y. Ishai and V. Rijmen, Eds. Cham: Springer International Publishing, 2019, pp. 375–403.

[10] S. De, L. Berrada, J. Hayes, S. L. Smith, and B. Balle, "Unlocking high-accuracy differentially private image classification through scale," *arXiv preprint arXiv:2204.13650*, 2022.

[11] J. Devlin, M. Chang, K. Lee, and K. Toutanova, "BERT: pre-training of deep bidirectional transformers for language understanding," in *Proceedings of the 2019 Conference of the North American Chapter of the Association for Computational Linguistics: Human Language Technologies, NAACL-HLT 2019, Minneapolis, MN, USA, June 2-7, 2019, Volume 1 (Long and Short Papers)*, J. Burstein, C. Doran, and T. Solorio, Eds. Association for Computational Linguistics, 2019, pp. 4171–4186. [Online]. Available: <https://doi.org/10.18653/v1/n19-1423>

[12] J. Dong, A. Roth, and W. Su, "Gaussian differential privacy," *Journal of the Royal Statistical Society*, 2021.

[13] A. Dosovitskiy, L. Beyer, A. Kolesnikov, D. Weissenborn, X. Zhai, T. Unterthiner, M. Dehghani, M. Minderer, G. Heigold, S. Gelly, J. Uszkoreit, and N. Houlsby, "An image is worth 16x16 words: Transformers for image recognition at scale," in *9th International Conference on Learning Representations, ICLR 2021, Virtual Event, Austria, May 3-7, 2021*. OpenReview.net, 2021. [Online]. Available: <https://openreview.net/forum?id=YicbFdNTTy>

[14] C. Dwork, F. McSherry, K. Nissim, and A. Smith, "Calibrating noise to sensitivity in private data analysis," in *Theory of cryptography conference*. Springer, 2006, pp. 265–284.

[15] U. Erlingsson, V. Feldman, I. Mironov, A. Raghunathan, K. Talwar, and A. Thakurta, "Amplification by shuffling: from local to central differential privacy via anonymity," in *Proceedings of the Thirtieth Annual ACM-SIAM Symposium on Discrete Algorithms*, ser. SODA '19. USA: Society for Industrial and Applied Mathematics, 2019, p. 2468–2479.

[16] V. Feldman, A. McMillan, and K. Talwar, "Hiding among the clones: A simple and nearly optimal analysis of privacy amplification by shuffling," in *2021 IEEE 62nd Annual Symposium on Foundations of Computer Science (FOCS)*, 2022, pp. 954–964.

[17] —, "Hiding among the Clones: A Simple and Nearly Optimal Analysis of Privacy Amplification by Shuffling," in *2021 IEEE 62nd Annual*

- Symposium on Foundations of Computer Science (FOCS)*. IEEE, 2022, pp. 954–964.
- [18] L. Fenton, “The sum of log-normal probability distributions in scatter transmission systems,” *IRE Transactions on Communications Systems*, vol. 8, no. 1, pp. 57–67, 1960.
- [19] A. Gohilkar, A. Achille, Y.-X. Wang, A. Roth, M. Kearns, and S. Soatto, “Mixed differential privacy in computer vision,” *2022 IEEE/CVF Conference on Computer Vision and Pattern Recognition (CVPR)*, pp. 8366–8376, 2022.
- [20] M. Gooneratne, K. C. Sim, P. Zadrazil, A. Kabel, F. Beaufays, and G. Motta, “Low-rank gradient approximation for memory-efficient on-device training of deep neural network,” *ICASSP 2020 - 2020 IEEE International Conference on Acoustics, Speech and Signal Processing (ICASSP)*, pp. 3017–3021, 2020.
- [21] S. Gopi, Y. T. Lee, and L. Wutschitz, “Numerical composition of differential privacy,” *Advances in Neural Information Processing Systems*, vol. 34, pp. 11 631–11 642, 2021.
- [22] J. He, X. Li, D. Yu, H. Zhang, J. Kulkarni, Y. T. Lee, A. Backurs, N. Yu, and J. Bian, “Exploring the limits of differentially private deep learning with group-wise clipping,” in *The Eleventh International Conference on Learning Representations*, 2023. [Online]. Available: <https://openreview.net/forum?id=oze0cIVGPeX>
- [23] S. Hoory, A. Feder, A. Tendler, S. Erell, A. Peled-Cohen, I. Laish, H. Nakhost, U. Stemmer, A. Benjamini, A. Hassidim, and Y. Matias, “Learning and evaluating a differentially private pre-trained language model,” in *Findings of the Association for Computational Linguistics: EMNLP 2021*. Punta Cana, Dominican Republic: Association for Computational Linguistics, Nov. 2021, pp. 1178–1189. [Online]. Available: <https://aclanthology.org/2021.findings-emnlp.102>
- [24] P. Kairouz, B. McMahan, S. Song, O. Thakkar, A. Thakurta, and Z. Xu, “Practical and private (deep) learning without sampling or shuffling,” in *Proceedings of the 38th International Conference on Machine Learning*, ser. Proceedings of Machine Learning Research, M. Meila and T. Zhang, Eds., vol. 139. PMLR, 18–24 Jul 2021, pp. 5213–5225. [Online]. Available: <https://proceedings.mlr.press/v139/kairouz21b.html>
- [25] A. Koskela and A. Honkela, “Computing differential privacy guarantees for heterogeneous compositions using fft,” 2021.
- [26] A. Koskela, J. Jälkö, and A. Honkela, “Computing tight differential privacy guarantees using fft,” pp. 2560–2569, 26–28 Aug 2020. [Online]. Available: <https://proceedings.mlr.press/v108/koskela20b.html>
- [27] A. Koskela, J. Jälkö, L. Prediger, and A. Honkela, “Tight differential privacy for discrete-valued mechanisms and for the subsampled gaussian mechanism using fft,” pp. 3358–3366, 13–15 Apr 2021. [Online]. Available: <https://proceedings.mlr.press/v130/koskela21a.html>
- [28] A. Krizhevsky, G. Hinton *et al.*, “Learning multiple layers of features from tiny images,” Citeseer, Tech. Rep., 2009.
- [29] A. Kurakin, S. Chien, S. Song, R. Geambasu, A. Terzis, and A. Thakurta, “Toward training at imagenet scale with differential privacy,” *CoRR*, vol. abs/2201.12328, 2022. [Online]. Available: <https://arxiv.org/abs/2201.12328>
- [30] T. Li, L. Tan, Z. Huang, Q. Tao, Y. Liu, and X. Huang, “Low dimensional trajectory hypothesis is true: Dnns can be trained in tiny subspaces,” *IEEE Transactions on Pattern Analysis and Machine Intelligence*, 2022.
- [31] X. Li, F. Tramer, P. Liang, and T. Hashimoto, “Large language models can be strong differentially private learners,” in *International Conference on Learning Representations*, 2022. [Online]. Available: <https://openreview.net/forum?id=bVuP3ltATMz>
- [32] I. Mironov, K. Talwar, and L. Zhang, “Rényi differential privacy of the sampled gaussian mechanism,” *CoRR*, vol. abs/1908.10530, 2019.
- [33] L. Nan, D. R. Radev, R. Zhang, A. Rau, A. Sivaprasad, C. Hsieh, X. Tang, A. Vyas, N. Verma, P. Krishna, Y. Liu, N. Irwanto, J. Pan, F. Rahman, A. Zaidi, M. Mutuma, Y. Tarabar, A. Gupta, T. Yu, Y. C. Tan, X. V. Lin, C. Xiong, R. Socher, and N. F. Rajani, “DART: open-domain structured data record to text generation,” in *Proceedings of the 2021 Conference of the North American Chapter of the Association for Computational Linguistics: Human Language Technologies, NAACL-HLT 2021, Online, June 6-11, 2021*, K. Toutanova, A. Rumshisky, L. Zettlemoyer, D. Hakkani-Tür, I. Beltagy, S. Bethard, R. Cotterell, T. Chakraborty, and Y. Zhou, Eds. Association for Computational Linguistics, 2021, pp. 432–447. [Online]. Available: <https://doi.org/10.18653/v1/2021.naacl-main.37>
- [34] M. Nasr, J. Hayes, T. Steinke, B. Balle, F. Tramèr, M. Jagielski, N. Carlini, and A. Terzis, “Tight auditing of differentially private machine learning,” in *32nd USENIX Security Symposium, USENIX Security 2023, Anaheim, CA, USA, August 9-11, 2023*, J. A. Calandrino and C. Troncoso, Eds. USENIX Association, 2023, pp. 1631–1648. [Online]. Available: <https://www.usenix.org/conference/usenixsecurity23/presentation/nasr>
- [35] J. Novikova, O. Dusek, and V. Rieser, “The E2E dataset: New challenges for end-to-end generation,” in *Proceedings of the 18th Annual SIGdial Meeting on Discourse and Dialogue, Saarbrücken, Germany, August 15-17, 2017*, K. Jokinen, M. Stede, D. DeVault, and A. Louis, Eds. Association for Computational Linguistics, 2017, pp. 201–206. [Online]. Available: <https://doi.org/10.18653/v1/w17-5525>
- [36] A. Radford, J. Wu, R. Child, D. Luan, D. Amodei, and I. Sutskever, “Language models are unsupervised multitask learners,” *OpenAI Blog*, vol. 1(8):9, 2019.
- [37] M. A. Rahman, T. Rahman, R. Laganière, and N. Mohammed, “Membership inference attack against differentially private deep learning model,” *Transactions on Data Privacy*, vol. 11, no. 1, pp. 61–79, 2018. [Online]. Available: <http://www.tdp.cat/issues16/tdp.a289a17.pdf>
- [38] A. Sablayrolles, M. Douze, C. Schmid, Y. Ollivier, and H. Jégou, “White-box vs black-box: Bayes optimal strategies for membership inference,” in *International Conference on Machine Learning*, 2019.
- [39] S. Song, K. Chaudhuri, and A. D. Sarwate, “Stochastic gradient descent with differentially private updates,” in *2013 IEEE Global Conference on Signal and Information Processing*. IEEE, 2013, pp. 245–248.
- [40] T. Steinke, “Composition of differential privacy & privacy amplification by subsampling,” *ArXiv*, vol. abs/2210.00597, 2022. [Online]. Available: <https://api.semanticscholar.org/CorpusID:252683292>
- [41] . Thijs Vogels, . Sai Praneeth Karimireddy, and M. Jaggi, “Powersgd: Practical low-rank gradient compression for distributed optimization,” in *Proceedings of the Advances in Neural Information Processing Systems (NeurIPS)*, 2019.
- [42] A. Vaswani, N. M. Shazeer, N. Parmar, J. Uszkoreit, L. Jones, A. N. Gomez, L. Kaiser, and I. Polosukhin, “Attention is all you need,” in *Neural Information Processing Systems*, 2017.
- [43] A. Wang, A. Singh, J. Michael, F. Hill, O. Levy, and S. R. Bowman, “GLUE: A multi-task benchmark and analysis platform for natural language understanding,” in *7th International Conference on Learning Representations, ICLR 2019, New Orleans, LA, USA, May 6-9, 2019*. OpenReview.net, 2019. [Online]. Available: <https://openreview.net/forum?id=rJ4km2R5t7>
- [44] C. Wang, B. Su, J. Ye, R. Shokri, and W. Su, “Unified Enhancement of Privacy Bounds for Mixture Mechanisms via f -Differential Privacy,” *Advances in Neural Information Processing Systems (NeurIPS)*, vol. 36, 2024.
- [45] T. Wolf, L. Debut, V. Sanh, J. Chaumond, C. Delangue, A. Moi, P. Cistac, T. Rault, R. Louf, M. Funtowicz, J. Davison, S. Shleifer, P. von Platen, C. Ma, Y. Jernite, J. Plu, C. Xu, T. L. Scao, S. Gugger, M. Drame, Q. Lhoest, and A. M. Rush, “Transformers: State-of-the-art natural language processing,” in *Proceedings of the 2020 Conference on Empirical Methods in Natural Language Processing: System Demonstrations*. Online: Association for Computational Linguistics, Oct. 2020, pp. 38–45. [Online]. Available: <https://www.aclweb.org/anthology/2020.emnlp-demos.6>
- [46] H. Xu, L. Xiang, H. Ye, D. Yao, P. Chu, and B. Li, “Permutation equivariance of transformers and its applications,” in *Proceedings of the IEEE / CVF Computer Vision and Pattern Recognition Conference*, 2024.
- [47] A. Yousefpour, I. Shilov, A. Sablayrolles, D. Testuggine, K. Prasad, M. Malek, J. Nguyen, S. Ghosh, A. Bharadwaj, J. Zhao, G. Cormode, and I. Mironov, “Opacus: User-friendly differential privacy library in pytorch,” in *NeurIPS 2021 Workshop Privacy in Machine Learning*, 2021. [Online]. Available: <https://openreview.net/forum?id=EopKEYBoI->
- [48] D. Yu, S. Naik, A. Backurs, S. Gopi, H. A. Inan, G. Kamath, J. Kulkarni, Y. T. Lee, A. Manoel, L. Wutschitz, S. Yekhanin, and H. Zhang, “Differentially private fine-tuning of language models,” in *International Conference on Learning Representations*, 2022. [Online]. Available: <https://openreview.net/forum?id=Q42f0dfjECO>
- [49] D. Yu, H. Zhang, W. Chen, and T.-Y. Liu, “Do not let privacy overbill utility: Gradient embedding perturbation for private learning,” in *International Conference on Learning Representations*, 2021.
- [50] D. Yu, H. Zhang, W. Chen, J. Yin, and T.-Y. Liu, “Large scale private learning via low-rank reparametrization,” in *International Conference on Machine Learning*. PMLR, 2021, pp. 12 208–12 218.

- [51] H. Zhang, I. Mironov, and M. Hejaziinia, “Wide network learning with differential privacy,” *CoRR*, vol. abs/2103.01294, 2021. [Online]. Available: <https://arxiv.org/abs/2103.01294>
- [52] X. Zhang, “A survey of the sum of lognormal distribution and some recent results,” Ph.D. dissertation, University of British Columbia, 2022. [Online]. Available: <https://open.library.ubc.ca/collections/ubctheses/24/items/1.0421709>
- [53] —, “A survey of the sum of lognormal distribution and some recent results,” Ph.D. dissertation, University of British Columbia, 2022. [Online]. Available: <https://open.library.ubc.ca/collections/ubctheses/24/items/1.0421709>
- [54] Y. Zhou, Z. S. Wu, and A. Banerjee, “Bypassing the ambient dimension: Private sgd with gradient subspace identification,” in *International Conference on Learning Representations*, 2021.
- [55] L. Zhu, Z. Liu, and S. Han, “Deep leakage from gradients,” in *Proc. of the Advances in Neural Information Processing Systems (NIPS)*, 2019.

A. Proof of Theorem 1

Proof. As we have

$$P(W) = \{P_1^\top W_t, b_t P_1, W_{t+1} P_1, b_{t+1}\}, \quad (46)$$

we can get the following equations by substituting the above into Eq. 3 and 4:

$$h(x_t W_t^\top P_1 + b_t P_1) = x_{t+1} P_1, \quad (47)$$

$$h(x_{t+1} P_1 P_1^\top W_{t+1}^\top + b_{t+1}) = x_{t+2}. \quad (48)$$

Therefore, the forwarding result is still x_{t+2} , satisfying forward invariance.

For the backward propagation, we can get the gradients as:

$$\frac{\partial x_{t+2}}{\partial W_{t+1} P_1} = \frac{\partial x_{t+2}}{\partial W_{t+1}} \frac{\partial W_{t+1}}{\partial W_{t+1} P_1} = \frac{\partial x_{t+2}}{\partial W_{t+1}} P_1, \quad (49)$$

$$\frac{\partial x_{t+2}}{\partial b_{t+1}} = \frac{\partial x_{t+2}}{\partial b_{t+1}} \quad (50)$$

$$\frac{\partial x_{t+2}}{\partial P_1^\top W_t} = \frac{\partial x_{t+2}}{\partial W_t} \frac{\partial W_t}{\partial P_1^\top W_t} = P_1^\top \frac{\partial x_{t+2}}{\partial W_t}, \quad (51)$$

$$\frac{\partial x_{t+2}}{\partial b_t P_1} = \frac{\partial x_{t+2}}{\partial b_t} \frac{\partial b_t}{\partial b_t P_1} = \frac{\partial x_{t+2}}{\partial b_t} P_1. \quad (52)$$

Therefore, the gradients have the same permutation order with the weights, and thus the results of the backward propagation are not changed. \square

B. Proof of Theorem 2

Proof. For the permuted attention block, we simplify the inner product of QK to get:

$$W_i^Q P_{1i} P_{1i}^\top W_i^{K^\top} = W_i^Q W_i^{K^\top}. \quad (53)$$

Hence, we get:

$$\text{softmax} \left(\frac{X_t W_i^Q W_i^{K^\top} X_t^\top}{\sqrt{d_k}} \right) X_t W_i^V P_2 = A_i P_2. \quad (54)$$

Combining A_i s together according to the definition of attention, and multiplying the result with W^O , we have:

$$[A_1 P_2, \dots, A_h P_2] P_3 W^O = [A_1, \dots, A_h] W^O = X_{t+1}. \quad (55)$$

Therefore, we can get the result of shuffling does not alter from the original one in the forwarding pass.

For the backward propagation, we get that the gradients as:

$$\frac{\partial X_{t+1}}{\partial W_i^Q P_{1i}} = \frac{\partial X_{t+1}}{\partial W_i^Q} \frac{\partial W_i^Q}{\partial W_i^Q P_{1i}} = \frac{\partial X_{t+1}}{\partial W_i^Q} P_{1i}, \quad (56)$$

$$\frac{\partial X_{t+1}}{\partial W_i^K P_{1i}} = \frac{\partial X_{t+1}}{\partial W_i^K} \frac{\partial W_i^K}{\partial W_i^K P_{1i}} = \frac{\partial X_{t+1}}{\partial W_i^K} P_{1i}, \quad (57)$$

$$\frac{\partial X_{t+1}}{\partial W_i^V P_2} = \frac{\partial X_{t+1}}{\partial W_i^V} \frac{\partial W_i^V}{\partial W_i^V P_2} = \frac{\partial X_{t+1}}{\partial W_i^V} P_2, \quad (58)$$

$$\frac{\partial X_{t+1}}{\partial P_3 W^O} = \frac{\partial X_{t+1}}{\partial W^O} \frac{\partial W^O}{\partial P_3 W^O} = P_3 \frac{\partial X_{t+1}}{\partial W^O}. \quad (59)$$

Therefore, the gradients share the same permutation order with the weights, demonstrating backward invariance in the weight update. \square

C. Proof of Theorem 6

Lemma 3. Assuming a_1, a_2, \dots, a_k and b_1, b_2, \dots, b_k are positive real numbers, we have

$$\sum_{i=1}^k a_i \sum_{i=1}^k b_i \geq \sum_{i=1}^k a_i b_i. \quad (60)$$

Proof. Obviously,

$$\sum_{i=1}^k a_i \sum_{i=1}^k b_i = \sum_{i=1}^k a_i b_i + \sum_{i \neq j} a_i b_j > \sum_{i=1}^k a_i b_i. \quad (61)$$

\square

Substituting Eq. (29) into the above inequality, we obtain

$$\frac{\sum_{i=1}^k e^{\langle y, f^{(i)} \rangle / \sigma^2}}{\sum_{i=1}^k e^{\langle y, f^{(i)} \rangle + \langle y, g^{(i)} \rangle / \sigma^2}} \geq \frac{1}{\sum_{i=1}^k e^{\langle y, g^{(i)} \rangle / \sigma^2}}. \quad (62)$$

Therefore, a sufficient condition for O^* is to have

$$\frac{1}{e^{-\langle \|g\|_2^2 + 2\langle f, g \rangle \rangle / (2\sigma^2)} \sum_{i=1}^k e^{\langle y, g^{(i)} \rangle / \sigma^2}} \geq e^\epsilon \quad (63)$$

$$\Leftrightarrow e^{-\epsilon + \langle \|g\|_2^2 + 2\langle f, g \rangle \rangle / (2\sigma^2)} \geq \sum_{i=1}^k e^{\langle y, g^{(i)} \rangle / \sigma^2}. \quad (64)$$

D. Proof of Lemma 2

Proof. In $h(\sigma_{Z_1}, \sigma_{Z_2}) = \Phi \left(\frac{\sigma_{Z_1}}{2} + \frac{\zeta_1 - \epsilon}{\sigma_{Z_1}} \right) - e^\epsilon \Phi \left(\frac{\sigma_{Z_2}}{2} + \frac{\zeta_2 - \epsilon}{\sigma_{Z_2}} \right)$, for the definitions of $\zeta_1, \zeta_2, \sigma_{Z_1}, \sigma_{Z_2}$, we can easily derive

$$\zeta_1 \leq 0, \quad \zeta_2 \leq \zeta_1 - \frac{\|g\|_2^2}{\sigma^2}, \quad (65)$$

$$\log \left[\frac{1}{k} \left(e^{\frac{\|g\|_2^2}{\sigma^2}} - 1 \right) + 1 \right] < \sigma_{Z_i}^2 < \frac{\|g\|_2^2}{\sigma^2}, \quad i = 1, 2. \quad (66)$$

By analysis, we found $h(\cdot)$ is mostly influenced by the term $\sum_{j=1}^k e^{2\mu_{ij}}, \sum_{j=1}^k e^{\mu_{ij}}, \sum_{j=1}^k e^{2\mu'_{ij}}$, and $\sum_{j=1}^k e^{\mu'_{ij}}$. Letting

$$\boldsymbol{\mu} = [e^{\mu_{i1}}, e^{\mu_{ik}}, \dots, e^{\mu_{ik}}] \in \mathbb{R}^k, \quad (67)$$

$$A = \text{diag} \left\{ e^{\frac{\langle g^{(i)}, g^{(1)} \rangle}{\sigma^2}}, e^{\frac{\langle g^{(i)}, g^{(2)} \rangle}{\sigma^2}}, \dots, e^{\frac{\langle g^{(i)}, g^{(k)} \rangle}{\sigma^2}} \right\} \in \mathbb{R}^{k \times k}, \quad (68)$$

one can rewrite the terms as

$$\sum_{j=1}^k e^{2\mu_{ij}} = \|\boldsymbol{\mu}\|_2^2, \quad \sum_{j=1}^k e^{\mu_{ij}} = \|\boldsymbol{\mu}\|_1 \quad (69)$$

$$\sum_{j=1}^k e^{2\mu'_{ij}} = \|A\boldsymbol{\mu}\|_2^2, \quad \sum_{j=1}^k e^{\mu'_{ij}} = \|A\boldsymbol{\mu}\|_1. \quad (70)$$

Substituting the above shorthand into the variables, we have

$$\sigma_{Z_1}^2 = \log \left[\frac{\|\boldsymbol{\mu}\|_2^2}{\|\boldsymbol{\mu}\|_1^2} (e^{\frac{\|g\|_2^2}{\sigma^2}} - 1) + 1 \right], \quad (71)$$

$$\sigma_{Z_2}^2 = \log \left[\frac{\|A\boldsymbol{\mu}\|_2^2}{\|A\boldsymbol{\mu}\|_1^2} (e^{\frac{\|g\|_2^2}{\sigma^2}} - 1) + 1 \right], \quad (72)$$

$$\zeta_1 = -\log(\|\boldsymbol{\mu}\|_1) + \frac{\langle f, g \rangle}{\sigma^2}, \quad (73)$$

$$\zeta_2 = -\log(\|A\boldsymbol{\mu}\|_1) + \frac{\langle f, g \rangle}{\sigma^2}. \quad (74)$$

Since $\sigma_{Z_1}^2$ and $\sigma_{Z_2}^2$ only appear in $h(\cdot)$ as square root magnitudes, their influence is relatively small compared to the changes in $\boldsymbol{\mu}$ and A . Therefore, we mainly consider the impact of ζ_1 and ζ_2 on h . It is not difficult to see that the larger the difference $\zeta_1 - \zeta_2$, the greater the value of the function h . Additionally, the larger ζ_1 is, the greater the value of the function h . Moreover, since $\|A\boldsymbol{\mu}\|_1 \leq \|A\|_1 \|\boldsymbol{\mu}\|_1$ holds by norm inequality, we have:

$$\zeta_2 \geq -\log \|A\|_1 - \log(\|\boldsymbol{\mu}\|_1) + \frac{\langle f, g \rangle}{\sigma^2} = \zeta_1 - \log \|A\|_1. \quad (75)$$

By the definition of A , we have $\|A\|_1 = e^{\frac{\|g\|_2^2}{\sigma^2}}$, since $e^{\frac{\|g\|_2^2}{\sigma^2}}$ is the maximal element in the diagonal of A . The largest gap between ζ_1 and ζ_2 is achieved at $\|A\boldsymbol{\mu}\|_1 = \|A\|_1 \|\boldsymbol{\mu}\|_1$ which holds under two conditions: 1) $A = e^{\frac{\|g\|_2^2}{\sigma^2}} E$, where E is the identity matrix; 2) $A\boldsymbol{\mu} = e^{\frac{\|g\|_2^2}{\sigma^2}} \boldsymbol{\mu}$, where $\boldsymbol{\mu}$ is an eigenvector of the matrix A corresponding to the eigenvalue $e^{\frac{\|g\|_2^2}{\sigma^2}}$. Below, we will discuss each case separately and determine the conditions to achieve the maximum value of h .

The first case implies that the inner products of $g^{(i)}$ and $g^{(j)}$ are all equal to $\|g\|_2^2$, which is almost impossible for $k > 1$. To exclude the case where every $g^{(i)}$ is close to the vector $[1, 1, \dots, 1]$, we ensure that in the high-dimensional space, the probability that the angle between $g^{(i)}$ and $[1, 1, \dots, 1]$ being less than $\pi/4$ is almost zero. Therefore, we will not consider this case here.

For the second case, it is clear that the eigenvectors of the diagonal matrix A are standard base vectors e_i which has a 1 in the i -th position and 0 elsewhere. Therefore, the vector $\boldsymbol{\mu}$ is close to the direction of one of these base vectors. According to the observation that the larger ζ_1 is, the larger the value of the function h will be, and thus we need to maximize ζ_1 .

Since

$$\zeta_1 = -\log \left(e^{\frac{\langle f, g \rangle}{\sigma^2}} + \sum_{j \neq i} e^{\frac{\langle f^{(i)}, g^{(j)} \rangle}{\sigma^2}} \right) + \frac{\langle f, g \rangle}{\sigma^2} \quad (76)$$

$$= -\log \left(\sum_{j=1}^k e^{\frac{\langle f^{(i)}, g^{(j)} \rangle - \langle f, g \rangle}{\sigma^2}} \right), \quad (77)$$

the larger $\langle f, g \rangle$ is, and the smaller $\langle f^{(i)}, g^{(j)} \rangle$ ($j \neq i$) is, the larger ζ_1 becomes. Moreover, as $\langle f^{(i)}, g^{(j)} \rangle$ is lower bounded by

$$e^{\mu_{ij}} = e^{\frac{\langle f^{(i)}, g^{(j)} \rangle}{\sigma^2}} \geq e^{-\frac{\|f\|_2 \|g\|_2}{\sigma^2}}, \quad (78)$$

the smaller the value of k , the larger ζ_1 is, with the minimum value of k being d . Therefore, given the constraints $\|g\|_2 \leq c$ and $\|f\|_2 \leq c'$, we reformulate the problem to maximize the following optimization problem:

$$\text{maximize } \sum_{j=1}^k (\langle f, g \rangle - \langle f^{(i)}, g^{(j)} \rangle). \quad (79)$$

Note that $\langle f, g \rangle$ is maximized when f and g are of the same direction. The original problem can be transformed into:

$$\text{maximize } k(\langle f, g \rangle - \langle f^{(i)}, \frac{1}{k} \sum_{j=1}^k g^{(j)} \rangle) \quad (80)$$

Since f and g are in the same direction, we must have $\langle f^{(i)}, \frac{1}{k} \sum_{j=1}^k g^{(j)} \rangle \geq 0$. When $\langle f^{(i)}, \frac{1}{k} \sum_{j=1}^k g^{(j)} \rangle = 0$, ζ_1 reaches its maximum value. In this case, since $\frac{1}{k} \sum_{j=1}^k g^{(j)}$ is parallel to $[1, 1, \dots, 1]$, and f and g are in the same direction, then $g \perp [1, 1, \dots, 1]$. Meanwhile, since $k = d$ when ζ_1 is maximized, g cannot be in any other form other than having one dimension different with the rest being the same. Combining the two criteria, we could solve g and f as

$$f = \sqrt{\frac{1}{d(d-1)}} c' [(d-1), -1, \dots, -1] \quad (81)$$

$$g = \sqrt{\frac{1}{d(d-1)}} c [(d-1), -1, \dots, -1]. \quad (82)$$

Under these conditions, we have

$$\zeta_1 = -\log(1 + (d-1)e^{-\frac{d c c'}{(d-1)\sigma^2}}),$$

$$\zeta_2 = -\log(1 + (d-1)e^{-\frac{d c(c+c')}{(d-1)\sigma^2}}) - \frac{c^2}{\sigma^2},$$

$$\sigma_{Z_1}^2 = \log \left[\frac{1 + (d-1)e^{-\frac{2 d c c'}{(d-1)\sigma^2}}}{(1 + (d-1)e^{-\frac{d c c'}{(d-1)\sigma^2}})^2} (e^{\frac{\|g\|_2^2}{\sigma^2}} - 1) + 1 \right],$$

$$\sigma_{Z_2}^2 = \log \left[\frac{1 + (d-1)e^{-\frac{2 d c(c+c')}{(d-1)\sigma^2}}}{(1 + (d-1)e^{-\frac{d c(c+c')}{(d-1)\sigma^2}})^2} (e^{\frac{\|g\|_2^2}{\sigma^2}} - 1) + 1 \right], \quad (83)$$

which complete the proof. \square

E. Python Code for Index Shuffling

def rearrange(matrix, row, column):

if row:

indices = torch.randperm(matrix.shape[0])
matrix = matrix[indices]

if column:

indices = torch.randperm(matrix.shape[1])
matrix = matrix[:, indices]

return matrix